Geodynamic reconstruction of an accreted Cretaceous back-arc basin in the Northern Andes

Carmen Braz[1], Maria Seton[1*], Nicolas Flament[1†], and R. Dietmar Müller[1]

[1]EarthByte Group, School of Geosciences, The University of Sydney, Sydney, New South Wales 2006, Australia

*Corresponding author: Maria Seton (maria.seton@sydney.edu.au)

[†]Now at: School of Earth and Environmental Sciences, University of Wollongong, Northfields Avenue NSW 2522, Australia.

Abstract

A complex history of subduction, back-arc basin formation, terrane accretion and transpressional shearing characterizes the evolution of the Caribbean and northern South American margin since Jurassic times. Quantitative plate tectonic reconstructions of the area do not include Jurassic-Cretaceous back-arc terranes of which there are both geological and geophysical observations. We developed a revised plate tectonic reconstruction based on geological observations and seismic tomography models to constrain the Jurassic-Cretaceous subduction history of eastern Panthalassa, along the western margin of the Caribbean region. This reconstruction considers the opening of a Northern Andean back-arc basin at 145 Ma, the Quebradagrande back-arc, closing at 120 Ma and followed by terrane accretion and northward translation along the South American margin starting at 100 Ma. This kinematic reconstruction is tested against two previously published tectonic reconstructions via coupling with global numerical mantle convection models using CitcomS. A comparison of modeled versus tomographically imaged mantle structure reveals that subduction outboard of the South American margin, lacking in previous tectonic models, is required to reproduce mid-mantle positive seismic anomalies imaged in P- and S-wave seismic tomography beneath South America, 500-2000 km in depth. Furthermore, we show that this subduction zone is likely produced by a back-arc basin that developed along the northern Andes during the Cretaceous via trench roll-back from 145 Ma and was closed at 100 Ma. The contemporaneous opening of the Quebradagrande back-arc basin with the Rocas Verdes back-arc basin in the southern Andes is consistent with a model that invokes return flow of mantle material behind a retreating slab and may explain why extension along the Peruvian and Chilean sections of the Andean margin did not experience full crustal break-up and back-arc opening during the late Jurassic-early Cretaceous Period.

Keywords: Andes; backarc basin; subduction; geodynamic modeling; Quebradagrande

1 Introduction

Subduction is a process characterized by retreating trenches and the descending of oceanic lithosphere into the mantle. In some cases, where a mantle wedge is present above the subducted slab, back-arc extension between the active volcanic arc/fore-arc and the remnant arc may result (Hawkins, 1995). While back-arc basins are observed in many of the world's ocean basins, the Western Pacific has particularly been dominated by intra-oceanic subduction and episodic back-arc basin formation since as early as Cretaceous times (e.g. Karig, 1971; Matthews et al., 2015; Schellart et al., 2006; Sdrolias et al., 2003). In contrast, in the Eastern Pacific, specifically along the South American margin, back-arc extension leading to seafloor-spreading has not occurred since the end of the Mesozoic, when it transitioned into a largely compressional margin experiencing crustal shortening and mountain building (Mpodozis and Ramos, 1990).

Back-arc basins appear to be relatively short-lived and episodic features of subduction zones, active for only ~10-30 Myr (Faccenna et al., 2001; Schellart et al., 2006). Why back-arc basin formation is spatially variable across subduction zones remains uncertain. Absolute motion of the overriding plate has been linked to the style of back-arc deformation, back-arc extension or compression occurring as the result of upper plate retreat and advance, respectively (Chase, 1978; Heuret and Lallemand, 2005). Recent numerical modelling has shown that back-arc extension occurs preferentially where slab widths are narrow, and close to lateral slab edges where rollback of the slab is greatest (Schellart et al., 2007; Schellart and Moresi, 2013; Stegman et al., 2006). These results agree with the large trench retreat velocities observed in association with present day back-arc extension (Heuret and Lallemand, 2005; Schellart et al., 2007; Sdrolias and Müller, 2006).

Schellart et al. (2007) also showed that wide subduction zones, as occurs along South America, are near stationary near their center, with trench retreat velocities increasing towards the slab edges, inducing back-arc extension. This is consistent with the distribution of Jurassic-Cretaceous back-arc basins along the western South American margin (Fig. 1). These range from "aborted" marginal basins to oceanic-floored back-arcs revealing a pattern of decreased crustal attenuation towards the center of the margin (Mpodozis and Ramos, 1990). The back-arc origins of the late Jurassic-aged Rocas Verdes ophiolites in the southernmost Andes and mid-Cretaceous transition to compressive deformation of the margin has been well constrained (e.g. Calderón et al., 2007; Dalziel et al., 1974; Stern and De Wit, 2003). Uncovering the tectonic history of the Northern Andes however has proven more challenging, because it is obscured by successive phases of extension, terrane accretion, and large magnitude dextral shearing as the result of interaction with the Pacific-derived Caribbean plate during Cenozoic times (Kennan and Pindell, 2009; Ramos, 2010; Sarmiento-Rojas et al., 2006). This includes the Alao and Quebradagrande Terranes of the Northern Andes, where limited reliable geochemical and radiometric data result in conflicting interpretations, which include mid-ocean ridge, back-arc, oceanic arc, continental arc, and ensiliac marginal basin origins for these units (Cochrane et al., 2014; González, 1980; Nivia et al., 2006; Spikings et al., 2015; Villagómez et al., 2011). Consequently, this possible Andean back-arc basin has been largely overlooked in tectonic reconstructions of the region.

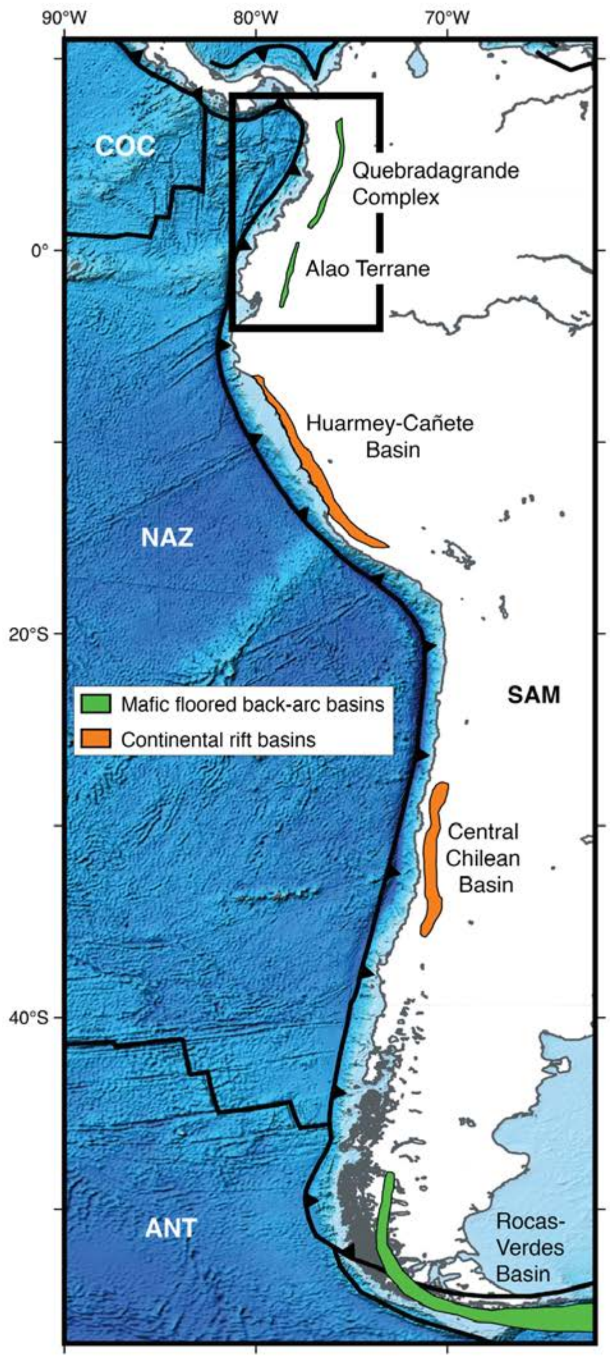

Figure 1. Basemap of seafloor bathymetry from ETOPO1 (Amante et al., 2009) with simplified boundaries of Cretaceous back-arc and extensional basins of the western South American margin (from Maloney et al., 2013). Present-day plate boundaries (Bird, 2003) are shown as thick black

lines. ANT: Antarctic Plate, COC: Cocos Plate, NAZ: Nazca plate, SAM: South American Plate. Black box shows the region in Figure 2.

Of the few studies that have considered a Cretaceous Andean back-arc basin (e.g. Kennan and Pindell, 2009; Pindell et al., 2012), none have ever been tested in a kinematic sense (i.e. in terms of Euler pole rotations and block outlines) or linked to the implied evolution of the surrounding plate margins, and in particular the evolution of the seafloor, in a self-consistent manner.

Seismic tomography studies have recently been used to identify seismically fast volumes in the mantle associated with past subduction systems (Domeier et al., 2016; Shephard et al., 2017; van der Meer et al., 2010; van der Meer et al., 2017). This approach has been particularly applied to North America where an analysis of the onshore geology coupled with seismic tomography images have indicated several generations of marginal and back-arc basins along this margin throughout the Mesozoic and early Cenozoic (Shephard et al., 2013; Sigloch and Mihalynuk, 2013). van Benthem et al. (2013) identified upper mantle slabs that indicate significant eastward motion of the Caribbean plate relative to the Americas since Eocene times. However, lower and mid-mantle anomalies evident in P- and S-wave tomography models beneath the northern South American margin, have yet to be extensively studied. Determining the origin of these anomalies can shed light on the subduction history of the Andean margin.

In areas where the geological history is heavily fragmented, as is the case in the Northern Andes, combining limited geological observations with seismic tomography and mantle convection models is useful to discriminate between alternative tectonic scenarios from predicted present-day mantle structure.

Here we combine onshore geological data, mantle tomography images and numerical models of past global mantle flow to investigate alternate geodynamic scenarios for the Cretaceous evolution of the northern Andes-Caribbean region. We develop a new plate kinematic and seafloor-spreading reconstruction of the northern Andean-Caribbean margin that considers the early-Cretaceous opening and mid-Cretaceous closure of a back-arc basin along the Andean margin. This reconstruction is used as time-dependent boundary condition in global numerical models of mantle flow. We compare the predicted regional thermal structure of the mantle to seismic tomography models for our tectonic model and two previous end-member scenarios (based on Ross and Scotese (1988) and Boschman et al. (2014)) and assess these results in the context of back-arc basin evolution.

2 Geological background

The northern Andes can be broadly divided into two geochemically distinct basement provinces, separated by a ~2,000 km tectonic suture that extends through the Ecuadorian and Colombian cordilleras (Villagómez et al., 2011). Allochthonous, ultramafic and mafic units define an oceanic province to the west of the Romeral Fault System, constituting the basement of the Western Cordillera and Cauca–Patía Valley in Colombia (Villagómez et al., 2011) (Fig. 2). This sequence is geochemically equivalent to the plateau basalts of the Caribbean Large Igneous Province (CLIP), having formed in an intra-oceanic hotspot setting during 99-87 Ma (Kerr et al., 1997; Spikings et al., 2015; Vallejo et al., 2006; Villagómez et al., 2011). The accretion of CLIP material is thought to have added at minimum 5.6 x 10^6 to 9.4 x 10^6 km^3 (Cochrane et al., 2014) of new crust to the South American margin at 75-73 Ma as a result of the collision of the eastward moving Caribbean plate with the northern Andean margin at this time (Vallejo et al., 2006; Vallejo et al., 2009). Within Ecuador, these rocks are represented by the Piñon, Palaltanga, and San Juan formations, whilst in Colombia they correspond to the Calima Terrane (Toussaint and Restrepo, 1994).

This accreted oceanic sequence is juxtaposed against the para-autochthonous and autochthonous units comprising an eastern continental province (Villagómez et al., 2011). The continental basement is interpreted to represent the southern passive paleo-continental margin of the Proto-Caribbean Sea, conjugate to the southeastern Chortis margin (Boschman et al., 2014; Villagómez et al., 2011). These units are comprised of Grenvillian-aged (~1.0 Ga) gneisses and schists, Paleozoic unmetamorphosed and metasedimentary rocks (Restrepo-Pace, 1992; Restrepo-Pace et al., 1997), overlain by a thin Cretaceous sedimentary cover sequence, intruded by plutons ranging in age from ~235-160 Ma (Kennan and Pindell, 2009; Villagómez et al., 2011).

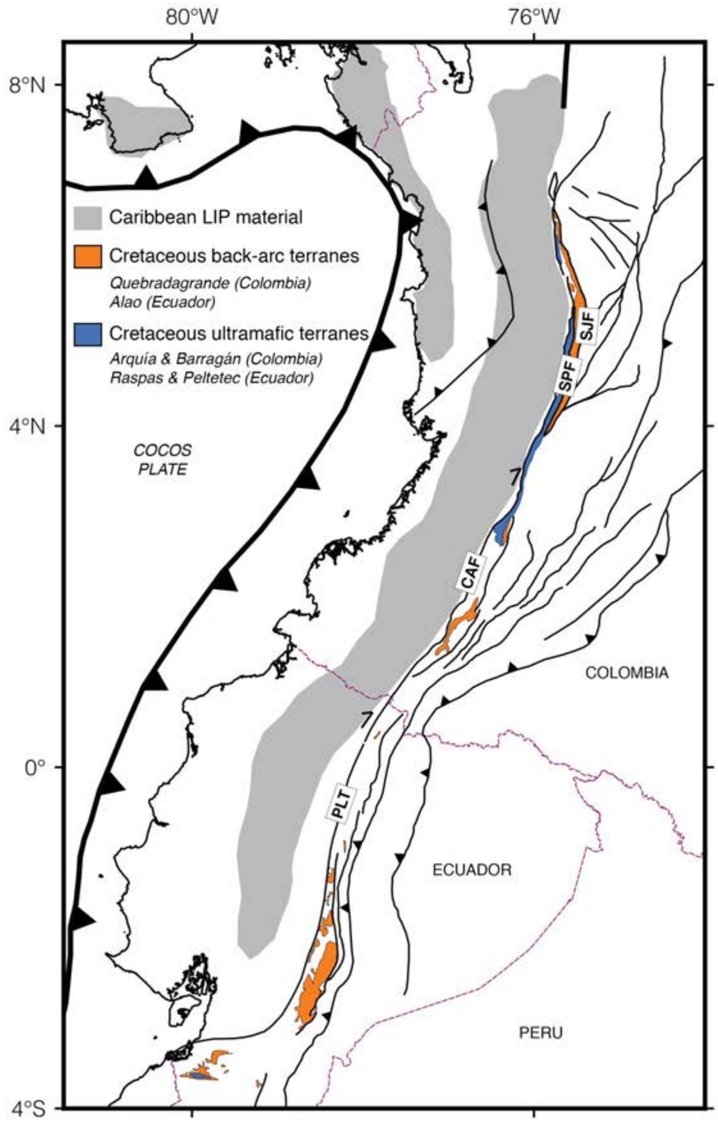

Figure 2. Terranes indicating back-arc extension and major fault systems of the northern Andes. CAF: Cauca–Almaguer Fault, PLT: Peltetec Fault, SJF: San Jerónimo Fault, SPF: Silvia–Pijao Fault. Terrane boundaries from Spikings et al. (2015).

In Colombia, the Romeral Fault System, interpreted as a tectonic suture zone, can be divided into three major branches: the San Jerónimo, Silvia–Pijao and Cauca–Almaguer Faults, that extend southwards merging with the Peltetec Fault zone in Ecuador (Villagómez et al., 2011).

Entrained within this fault system are the Quebradagrande and Arquia complexes, of central importance to this study (Fig. 2). The origin of these units is debated, with interpretations including mid-ocean ridge (González, 1980), oceanic arc (Villagómez et al., 2011), continental arc (Cochrane et al., 2014) and ensiliac marginal basin (Nivia et al., 2006).

Lithologies of the Quebradagrande Complex are dominated by low-grade metamorphosed gabbros, diorites, basalts, andesites, and pyroclastics (Nivia et al., 2006; Villagómez et al., 2011), covered by marine and terrestrial rocks of the Abejorral Formation which host Hauterivian to lower Albian fossils (González, 1980). These units are bound to the east by the San Jerónimo fault, juxtaposed against the Triassic-Paleozoic continental rocks of the Central Cordillera. The Quebradagrande Complex is considered to be coeval with the undated Alao Arc of Ecuador, displaying a similar structural position relative to the continental basement (Spikings et al., 2015; Villagómez et al., 2011). Moreno-Sanchez and Pardo-Trujillo (2003) collectively referred to these units as the Quebradagrande-Alao complex. Mora-Bohórquez et al. (2017) identified an oceanic terrane within the Lower Magdalena Valley, which they considered to be the northward continuation of the Quebradagrande terrane.

Limited geochemical studies of the igneous units that comprise the Quebradagrande and Alao sequences suggest that these rocks formed in a variety of tectonic environments, spanning calk-alkaline to tholeiitic compositions (Nivia et al., 2006; Spikings et al., 2015; Villagómez et al., 2011). Early radiometric dating of the suspect terranes of the Northern Andes region relied on K/Ar and Rb/Sr dating methods. However, partial resetting of the Rb/Sr and K/Ar isotopic systems and daughter isotope loss as a consequence of a sustained active margin through to the present day, led Spikings et al. (2015) to consider these studies unreliable. Villagómez et al. (2011) and Cochrane (2013) reported concordant zircon U-Pb dates of magmatic rocks of the Quebradagrande

Complex of 114.3 ± 3.8 Ma (tuff) and 112.9 ± 0.8 Ma (diorite) which overlaps with the Hautevarian-early Albian fossil ages for this unit (González, 1980).

To the west along the Silvia–Pijao fault, the Quebradagrande complex is in faulted contact with garnet-bearing amphibolites and lawsonite-glaucophane schists that constitute the Arquía and Barragán sequences (Spikings et al., 2015; Villagómez et al., 2011). Villagómez et al. (2011) and Spikings et al. (2015) suggested that the Arquía and Barragán complexes are the along-strike equivalent of the Raspas and Peltetec complexes in Ecuador, consisting of oceanic crust that mainly formed at a mid-ocean ridge, which was subsequently metamorphosed to high-to medium P-T conditions in an east-dipping subduction zone that gave rise to the Quebradagrande complex. Recent work conclude that variation in LREE enrichment, magmatic composition, and detrial zircon ages within the Quebradegrande complex can be explained by its formation over thin continental and newly formed oceanic back-arc related crust (Jaramillo et al., 2017).

Spikings et al. (2015) suggested that trench roll back and extension of the continental crust during ~145-114 Ma would have been sufficient to generate mafic magmas of T-MORB affinity and marine environments, consistent with the geological characteristics of the Quebradagrande and Alao complexes. Kennan and Pindell (2009) referred to this extensional feature as the "Colombian Marginal Seaway", a wide back-arc basin that formed a southward propagating arm of the Proto-Caribbean. This is consistent with the timing of a latest Jurassic–Hauterivian (144-127 Ma) extensional event identified by (Sarmiento-Rojas et al., 2006) in the Eastern Cordillera of Columbia. Additionally, Early Cretaceous intrusions in the Eastern Cordillera are attributed to rifting by Vásquez and Altenberger (2005). The width of the Colombian marginal Seaway and total orthogonal displacement of the Quebradagrande arc relative to South America is unknown. Villagómez et al. (2011) suggested that the T-MORB crust of the Quebradagrande Arc formed the relict basement of the Colombian Marginal Seaway and was originally entrained between the arc rocks and the continental terranes but has since been displaced.

Villagómez et al. (2011) proposed that $^{40}Ar/^{39}Ar$ ages of 117-107 Ma obtained in the Arquía complex (Villagómez Diaz, 2010) represent cooling ages during retrogression from peak metamorphic conditions. These ages are interpreted to correspond with the obduction, exhumation and accretion of the Arquía complex onto the Quebradagrande Arc and the continental margin in a compressive event that closed the Quebradagrande basin (Sarmiento-Rojas et al., 2006). This compression has been attributed to increased westward motion of the South American continent as a consequence of the opening of the South Atlantic during mid-Cretaceous times (Eagles, 2007; Ramos, 2010).

2.1 Peruvian Andes

South of the Huancacamba deflection, there is also evidence of back-arc extension recorded in the West Peruvian Trough (WPT), a major depositional structure that includes the north-south trending Casma-Huarmey and Canete Basins (Atherton and Aguirre, 1992; Cobbing, 1978). However, there have been few studies of the geochemistry and age of these basins.

These basins are thought to have opened during Tithonian times, experiencing maximum subsidence during Albian times, during which up to 9,000 m of basinal fill accumulated (Atherton and Aguirre, 1992; Atherton and Webb, 1989). The thick marine volcanic fill of the Casma-Huarmey Basin consists of pillow and sheet lavas, tuffs, hyaloclastites, and volcaniclastics associated with dyke swarms, sills and gabbros (Atherton, 1990; Petford and Atherton, 1994). A clear trend towards increasingly LIL and LREE depleted basalts towards the top of the basin is attributed to extensive crustal thinning, ultimately leading to the generation of new tholeiitic oceanic crust (Atherton and Webb, 1989; Petford and Atherton, 1994). A comparison of the Casma-Huarmey Basin facies with modern basin settings lead Atherton and Webb (1989) to suggest that the basin developed in a relatively isolated deep-sea environment with no continental input, characterised by a slow mid-ocean ridge (MOR) spreading system. The extent of crustal thinning is debated, with some researchers suggesting that extension did not occur on the scale required for the generation of new oceanic crust in this region, and are instead referred to as "aborted" marginal basins (Mpodozis and Allmendinger, 1993; Soler and Bonhomme, 1990).

Crustal extension in the southern part of the WPT was not as extensive and did not result in the development of new oceanic crust. The southern Cañete Basin developed on the Precambrian Arequipa Massif, thinning along southward propagating faults (Atherton and Aguirre, 1992). The bimodal calc-alkaline rocks that characterize the volcanic fill of this basin are sourced from enriched mantle beneath the Arequipa Massif, contrasting tholeiitic basalts of equivalent age in the Huarmey Basin to the north (Atherton and Aguirre, 1992). The Cretaceous collapse and closure of these back-arc basins along the Andean margin are attributed to the opening of the South Atlantic and subsequent westward motion of the South American plate (Mpodozis and Allmendinger, 1993). However, in a recent study, the change from extension and back-arc basin opening to shortening and back-arc basin closure has been ascribed to the change from upper mantle subduction to whole mantle subduction along the South American subduction zone (Schellart, 2017).

3 Plate tectonic reconstructions

3.1. Previous reconstructions

The evolution of the Northern Andes has been strongly influenced by the interaction of the margin with the Caribbean plate during Cenozoic times (Kennan and Pindell, 2009).

Ross and Scotese (1988) were amongst the first to use studies of the spreading history of the Cayman Trough derived from magnetic anomaly data (Rosencrantz et al., 1988; Ross et al., 1986) to constrain the mid-Eocene to present day motion of the Caribbean plate. The Cayman Trough represents one of the few elements of the Caribbean that can be reconstructed with a reasonable level of certainty, due to its preserved magnetic lineations, and is therefore consistently reconstructed across multiple studies. Magnetic anomalies elsewhere in the Caribbean are sparse due to the eruption of mantle plume derived basalts at 91-88 Ma (Sinton et al., 1998), forming the Caribbean Large Igneous Province (CLIP) (Fig. 3). The thickened crust of the Caribbean Sea is attributed to this event, effectively covering the spreading history of much of the Caribbean Sea with these volcanic rocks.

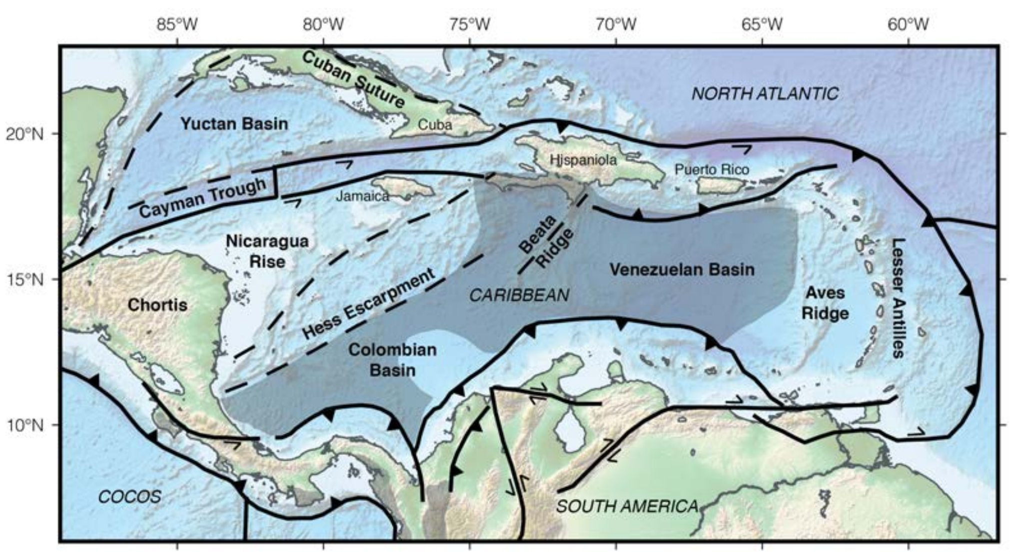

Figure 3. Present-day plate boundaries and major faults of the Caribbean region (Pindell and Kennan, 2009; Serrano et al., 2011; Villagómez et al., 2011). The extent of the Caribbean Large Igneous Province (CLIP) is shown in grey.

This has led to the rise of a variety of competing tectonic interpretations that can largely be divided into two end-member scenarios for the origin of the Caribbean plate: an "Intra-Americas origin" (James, 2005, 2009; Meschede and Frisch, 1998) and the more widely supported "Pacific origin" (Bouysse, 1988; Duncan and Hargraves, 1984; Kennan and Pindell, 2009; Müller et al., 1999; Nerlich et al., 2015; Pindell and Dewey, 1982; Pindell et al., 2012; Pindell and Barrett, 1990; Pindell and Kennan, 2009; Ross and Scotese, 1988; Whattam and Stern, 2015).

The accretion of oceanic plateau basalt and island arc terranes along the northwestern Andes combined with large magnitude dextral shear is best explained by the interaction of the Andean margin with the Great Arc of the Caribbean that formed at the leading edge of the Caribbean plate (Kennan and Pindell, 2009), a central component of "Pacific origin" models. Volcanic arc material and high-pressure, low-temperature (HP-LT) metamorphic rocks found along the circum-Caribbean margin, from Central America to the Aves Ridge and Lesser Antilles, and the Greater Antilles, including Cuba, Jamaica, Hispaniola and Puerto Rico are interpreted as the remnants of this former volcanic arc, initially forming at the subduction boundary between the future Caribbean plate and Proto-Caribbean Ocean (Burke, 1988). Pindell et al. (2012) suggest this arc first formed above a southwest dipping subduction zone at ~135 Ma, along an existing sinistral 'inter-American' transform, which previously connected the North and South American Cordilleras. The oldest magmatic arc rocks attributed to the Great Arc dated at ~132 Ma in the Devils Racecourse Formation, Jamaica (Hastie et al., 2009) and ~133 Ma in the Mabujina

Amphibolite Complex, Cuba (Rojas-Agramonte et al., 2011). The oldest reported single cooling age of HP-LT rocks of the Caribbean dates back to 118 Ma in the northern ophiolite belt of Central Cuba, indicating the minimum age of eclogite facies metamorphism (García-Casco et al., 2006). Following the inferences of Gerya et al. (2002), Pindell et al. (2012) suggest that the time lag between the ages of arc magmas and HP-LT rocks of the Caribbean is indicative of return flow from great depths in a mature subduction system, and therefore represent formation at the same subduction zone.

Alternative interpretations include those of Duncan and Hargraves (1984), Burke (1988) and Kerr et al. (2003) who suggested that the buoyant crust of the Caribbean Plateau blocked an earlier eastward dipping subduction zone inducing a subduction polarity reversal during Santonian-Campanian times (~85-80 Ma). This process would precipitate the eastward movement of Farallon lithosphere, which would eventually form the Caribbean plate, into the gap between the Americas. However, this model fails to explain evidence of Caribbean-northern Andean convergence already underway before 90 Ma (Kennan and Pindell, 2009).

Only two tectonic studies provide the Euler rotations that make them directly comparable to other models, those of Ross and Scotese (1988) and Boschman et al. (2014).

The model of Ross and Scotese (1988) was the first to approach Caribbean evolution in a quantitative sense, applying a hierarchical method to describe relative motion between pairs of tectonic components in terms of finite rotation poles. In this model, the Proto-Greater Antilles, analogous to the Great Arc of the Caribbean, originates at a subduction zone between the Farallon plate and the Proto-Caribbean between 143-100 Ma. The model includes a polarity reversal at the subduction zone beneath the Proto-Greater Antilles at ~100 Ma, allowing the advance of the Farallon plate into the widening gap between North and South America. Collision of the Great Arc with the Bahamas platform during the latest Cretaceous-earliest Paleocene is thought to have prohibited further eastward movement of Farallon lithosphere prompting the inception of eastward dipping subduction at 70 Ma, thus isolating the Caribbean plate. A recent tectonic model by Nerlich et al. (2015) presented an update of the Ross and Scotese (1988) model to include a younger age of collision between the Caribbean Plateau and the Proto-Greater Antilles Arc to 84 Ma.

Boschman et al. (2014) alternatively proposed an earlier age of initial westward-directed subduction below the Great Arc of the Caribbean at 135 Ma, given the oldest arc related units in the Caribbean date back to 133 Ma (Rojas-Agramonte et al., 2011) and HP-LT metamorphic blocks in the Cuban serpentinite mélange ranging from ~130 to 60 Ma (Somin et al., 1992).

3.2 Reconstructions in this Study

We create a self-consistent, dynamically evolving plate kinematic model of the Jurassic-Cretaceous Caribbean-northern Andean margin, which we embed into the global model of Müller et al. (2016) (Fig. 4). Müller et al. (2016) included a relative plate motion model for the Caribbean based on Boschman et al. (2014) and a hybrid absolute reference frame, combining a moving hotspot model since 100 Ma and a true-polar wander corrected paleomagnetic model for 200 to 100 Ma (see Müller et al. (2016)). The plates are modelled as dynamically closing polygons through time, defined by a series of intersecting plate boundaries, following the methodology outlined in Gurnis et al. (2012). For comparison, we have also developed continuously closing plate polygons for the regional reconstructions of Ross and Scotese (1988) and Boschman et al. (2014), which have been integrated into the global reconstructions by Seton et al. (2012) and by Müller et al. (2016), respectively. Companion paleo-seafloor age rasters (see Müller et al. (2008)

for further explanation) have been computed for all three reconstructions. These global maps of past seafloor ages are an important boundary condition for our geodynamic models as they allow us to reconstruct the thickness of the thermal oceanic lithosphere assuming a half-space cooling model.

Our reconstruction modifies the Early Cretaceous rotations of Boschman et al. (2014) by implementing the opening and closure of a Cretaceous back-arc basin system, the Quebradagrande back-arc basin, consistent with the geological record from the western Caribbean and northern South America. Corresponding Northern Andes arc material is modelled in Boschman et al. (2014) however its placement at a transform boundary is not consistent with its interpreted arc origin. We therefore modified the rotations of this block to a position along a retreating subduction zone outboard of South America, from 145 Ma (Fig. 4). We modelled this back-arc as a southern arm of the Proto-Caribbean spreading between North and South America, consistent with the Colombian Marginal Seaway of Kennan and Pindell (2009). Previous schematics of this back-arc basin (Kennan and Pindell, 2009; Pindell et al., 2012; Pindell and Kennan, 2009) show a back-arc basin of limited extent, ~200-300 km wide, and close to the margin. As little evidence is available to constrain the width of the basin, we used the boundary defined by Boschman et al. (2014) to constrain the western extent of paleo-location of back-arc subduction.

Additionally, we considered areas further south than what was considered in Boschman et al. (2014) and Ross and Scotese (1988), incorporating further evidence of back-arc basin formation in the West Peruvian Trough as described by Atherton and Aguirre (1992), Petford and Atherton (1994), and Ramos (2010). Full breakup and oceanic crust production are only proposed to have occurred in the northern region of the West Peruvian Trough, contrasting the primarily continental extensional setting of the southern basins. We constrained the north-south extent of the back-arc basin to reflect these differing rates of extension, reaching a maximum extent in the northern region of the back-arc, bending inwards towards the continental margin towards the south. The connection between the northern boundaries of our back-arc and the western North American margin are uncertain and beyond the scope of this study. However, the back-arc basin may have extended further north, adjacent to western North America, considering both geologic and seismic tomography evidence for intra-oceanic subduction outboard of the western North American margin (Sigloch and Mihalynuk, 2013).

As a consequence of westward-dipping subduction of the Proto-Caribbean initiating at 135 Ma to accommodate the formation of the Great Arc of the Caribbean, spreading of the Quebradagrande back-arc reverts to a two-plate system (Fig. 4). The back-arc basin was modelled to close from 119 Ma in response to the opening of the South Atlantic and northwest movement of the South American continent at this time (Spikings et al., 2015), with a reversal in the polarity of the subduction zone. Closure of the back-arc was finalized at 100 Ma (Kennan and Pindell, 2009), accompanied by the accretion of back-arc material to the South American margin (Villagómez et al., 2011) (Fig. 4). At this point, translation of the accreted terranes occurred along the Northern Andes, rotating to a position along the north-western Andean margin consistent with Boschman et al. (2014) by 85 Ma. From 85 Ma the new model retains the rotations of Boschman et al. (2014).

The spontaneous appearance of the Caribbean plate in eastern Panthalassa at 135 Ma, isolated by an unknown western plate boundary in Boschman et al. (2014) (Fig. 4) presents a kinematic problem. The eastward motion of the Farallon plate relative to this boundary requires the presence of eastward dipping subduction below the newly formed Caribbean plate, for which there is no geological evidence. Santonian–Campanian boninites, closely related to subduction initiation, are found in the accreted Greater Panama terranes in the Northern Andes (Kennan and Pindell, 2009). Therefore, we only isolated the Caribbean plate at 85 Ma, trapping Farallon oceanic lithosphere with the inception of an eastward dipping subduction zone.

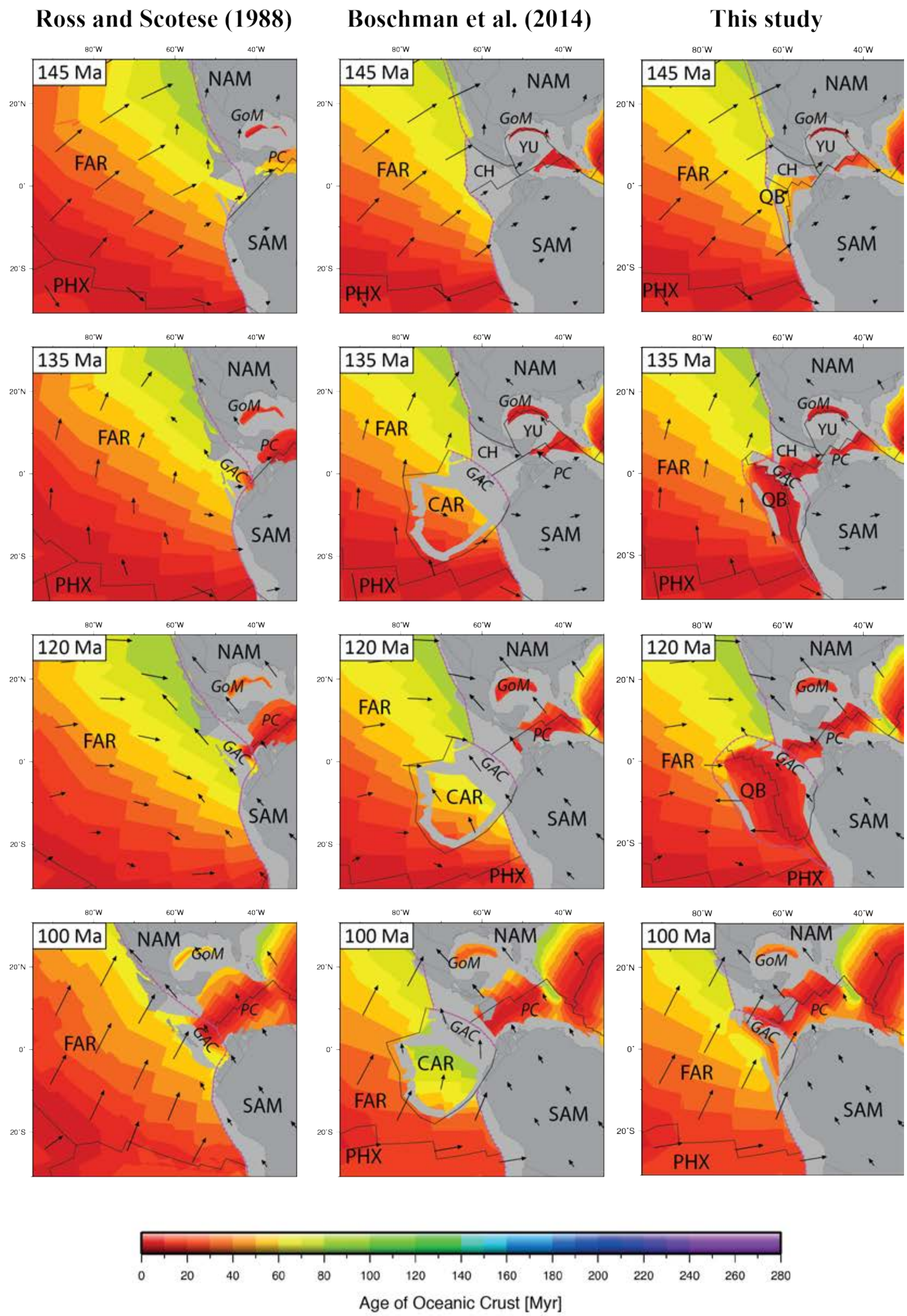

Figure 4. Reconstructions of Ross and Scotese (1988) (left), Boschman et al. (2014) (middle) and this study (right) from 145 to 100 Ma. Plate boundaries are defined as thin magenta lines for

subduction zones (with triangles on the overriding plate) and thin black lines defining either mid-ocean ridges or transform faults. In the case of the Boschman et al. (2014) reconstruction, the thin black lines along the northwestern, western and southern boundaries of the Caribbean plate denote undefined plate boundaries. Computed paleo-seafloor ages and absolute plate velocities are also plotted. CAR: Caribbean plate, CH: Chortis, FAR: Farallon plate, GAC: Great Arc of the Caribbean, GoM: Gulf of Mexico, NAM: North America, PHX: Phoenix plate, P-C: Proto-Caribbean, QB: Quebradagrande back-arc basin, SAM: South America, YU: Yucatan.

4. Geodynamic models

We ran a series of global forward numerical models of mantle flow that use plate kinematic data as surface boundary conditions to predict the present day thermal structure of the mantle. We used the finite element code *CitcomS* (Zhong et al., 2008), modified by Bower et al. (2015) to assimilate the time-dependent structure of the thermal lithosphere and of the shallow part of subducting slabs.

The mantle was considered to be an incompressible viscous fluid within a spherical shell, divided into 12 'caps', each extending from the surface to the core mantle boundary. We used ~ 13 million nodes to achieve a lateral average resolution of ~ 50 km at the surface and ~ 28 km at the core-mantle boundary, and a radial resolution of ~ 15 km near the surface, ~ 100 km at mid-mantle depths and ~ 27 km near the core-mantle boundary.

Convective vigor is determined by the Rayleigh number

$$Ra = \frac{\alpha_0 \rho_0 g_0 \Delta T h_M^3}{\kappa_0 \eta_0}$$

where α_0 is the coefficient of thermal expansivity, ρ_0 the density, g_0 the acceleration of gravity, ΔT the temperature change across the mantle, h_M is the depth of the mantle, κ the thermal diffusivity, η the viscosity.

Viscosity depends on temperature and depth following:

$$\eta = \eta_0(r)\exp\left(\frac{E_\eta}{R(T+T_\eta)} - \frac{E_\eta}{R(T_b+T_\eta)}\right)$$

where η is the viscosity, $\eta_0 = 1 \times 10^{21}$ Pa s is the reference viscosity, $E_\eta \approx 100$ kJ mol^{-1} (upper mantle) or $E_\eta \approx 33$ kJ mol^{-1} (lower mantle) is the activation energy, $R = 8.31$ J mol^{-1} K^{-1} is the universal gas constant, T is the dimensional temperature between 273 K and 3098 K, $T_b = 1685$ K is the background temperature of the mantle, $T_\eta = 452$ K is a temperature offset (Flament et al., 2014). The spherical mantle shell is radially divided into four layers: lithosphere (0-160 km), asthenosphere (160-310 km), upper mantle (310-660 km), and lower mantle (660-2867 km). A viscosity contrast of 100 between the upper and lower mantle was implemented in our model runs, consistent with the findings of Alpert et al. (2010), and the asthenosphere was assumed to be 10 times less viscous than the upper mantle (Fig. 5). Note that the thermal thickness of the oceanic lithosphere depends on its age according to the half-space cooling model (Bower et al., 2015). In the continents, the thermal thickness of the lithosphere depends on tectonothermal age (Archean lithosphere is 250 km thick, Proterozoic lithosphere 165 km thick, and Phanerozoic lithosphere 135 km thick; (Flament et al., 2014)). In addition, the reference viscosity is assumed to be 100 times larger between 0-160 km depth than between 310-660 km depth (upper mantle).

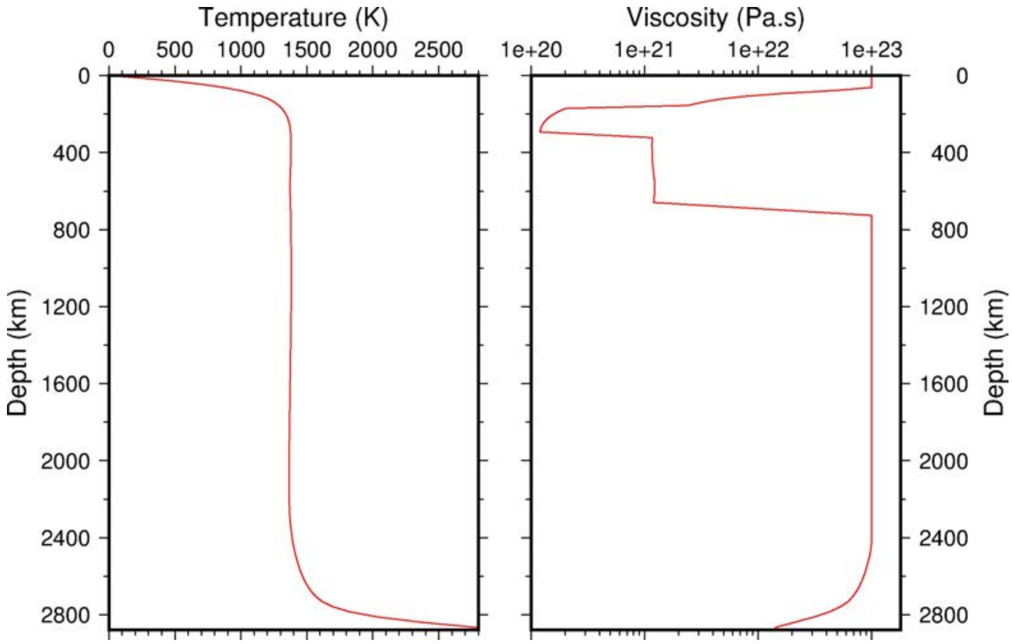

Figure 5. Horizontally-averaged present-day temperature and resulting viscosity profile.

In the initial condition at 230 Ma, subducted slabs derived from the tectonic reconstructions for each case are inserted down to 1,400 km depth, with a dip of 45° down to 425 km and a dip of 90° below this. Subduction zones thought to have initiated with insufficient time prior to 230 Ma to produce slabs at this depth (~85 Myr) were inserted to a depth based on subduction duration and a descent rate of 3 cm yr^{-1} in the upper mantle, and 1.2 cm yr^{-1} in the lower mantle (van der Meer et al., 2010). The main uncertainty in the location of subduction zones during the time period of our reconstructions is the absolute reference frame. The model of Müller et al. (2016) upon which our model is built, uses a global moving hotspot model (Steinberger et al., 2004) that is the most reasonable based on an evaluation of its global consistency with both hotspot trails and other geodynamic criteria (Williams et al., 2015) and produces similar results to the subduction reference frame of van der Meer et al. (2010). In addition, recent results have demonstrated that the lower mantle structure predicted by geodynamic models using the same base model as in our study is broadly consistent with seismic tomography images of the lower mantle (Flament et al., 2017), and thus provide us with a level of confidence in the plate models that are used in this study.

The initial mantle structure also includes a basal thermochemical layer 113 km thick (2% of the volume of the mantle following Hernlund and Houser (2008)) just above the core-mantle boundary that consists of material 3.6 % denser than ambient mantle (Flament et al., 2015).

4.1 Modelled mantle evolution

4.1.1 Ross and Scotese (1988)

In the absence of subduction outboard of the South American margin during Cretaceous times, the thermal structure of the mantle based on the reconstructions of Ross and Scotese (1988) is largely controlled by prolonged east-dipping subduction of Farallon (FAR) lithosphere beneath South America at 55°W. A vertical cross section at 4°S shows that this occurs continuously from 150 Ma to the present day, subducting as part of the Nazca plate from 23 Ma onwards (Fig. 6). As subduction remained uninterrupted along the South American margin, the subducted lithosphere remained attached to the base lithosphere through time. Increased westward motion of the South American continent associated with the opening of the Atlantic at ~120 Ma (Eagles, 2007), resulted in a ~30° westward relocation of the subduction zone from 120 Ma to the present day. As the subduction zone moved westward, subducted lithosphere in the upper and mid mantle was dragged with it, resulting in the diagonal smearing apparent in the predicted present-day mantle temperature cross-section. A gap opened in the subduction zone between 9 Ma and the present day. We see this mantle structure replicated at latitudes up to ~5°N. However, beneath the present-day Caribbean

Sea, subduction influx from both the Atlantic/Proto-Caribbean and Pacific realms is evident and is broadly similar between the considered geodynamic models.

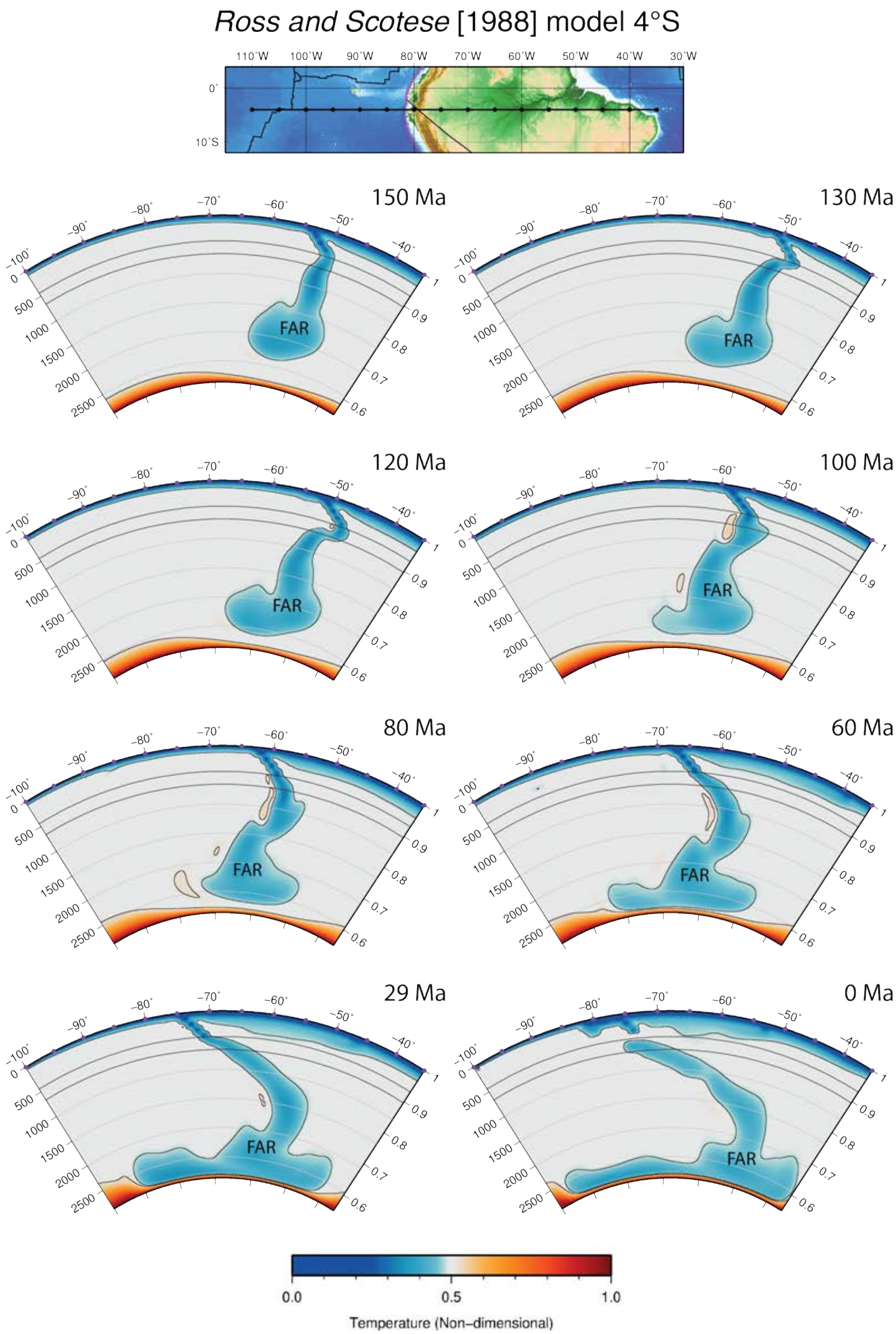

Figure 6. Vertical cross sections of time-dependent predicted mantle temperature based on the reconstruction Ross and Scotese (1988) at 4°S. Black contours correspond to material that is 4% cooler than ambient mantle temperature. FAR: Farallon oceanic lithosphere subducted beneath the South American continental margin.

4.1.2 Boschman et al. (2014)

The predicted thermal structure of the mantle is markedly different if a subduction zone is considered outboard of South America. The earlier onset of westward dipping subduction of Proto-Caribbean (PC) lithosphere beneath the Great Arc modelled by Boschman et al. (2014) resulted in the detachment of the Farallon slab (FARa) from the surface at 130 Ma (Fig. 7). By 120 Ma, subduction of the Farallon plate (FARb) began beneath the western trailing edge of the Caribbean plate at ~80°W. This subduction was not a feature of the reconstruction by Boschman et al. (2014) but was required because of the relative motion of the Farallon plate and Caribbean plate at this time.

With the eastward advance of the Caribbean plate, FARb was initially smeared laterally across the mantle transition zone from ~85-75°W. This volume only began to sink vertically into the lower mantle when it became detached by 59 Ma, eventually sinking to ~1500-2300 km depth at the present day. The additional slab material present at 150 Ma in the upper mantle at ~70°W was not associated with western Caribbean or Andean margin. It was instead related to the Jurassic Talkeetna-Bonanza subduction zone, associated with the closure of the Cache Creek (CC) Ocean and accretion of the Cache Creek terrane to the North American continent at ~180-150 Ma (Johnston and Borel, 2007). The southward extent of the Cache Creek Ocean was changed between the reconstruction of Seton et al. (2012) and that of Müller et al. (2016), hence why it was observed in the models that use the Müller et al. (2016) reconstructions.

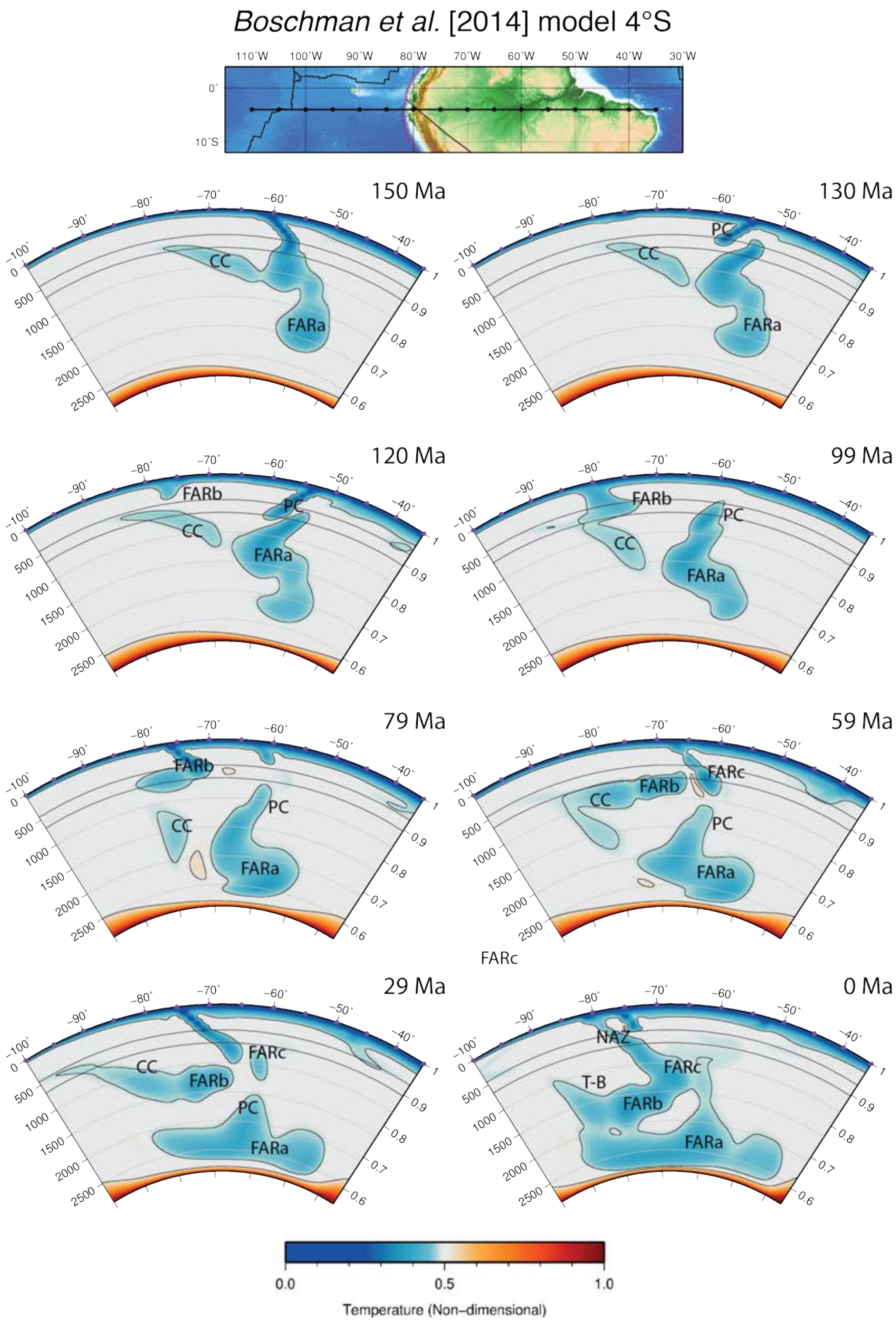

Figure 7. Vertical cross sections of time-dependent predicted mantle temperature based on the reconstruction Boschman et al. (2014) at 4°S. Black contours correspond to material that is 4%

cooler than ambient mantle temperature. FARa; Farallon lithosphere subducted below South America; CC; Cache Creek plate, PC; Proto-Caribbean lithosphere subducted below Caribbean plate, FARb; Farallon lithosphere subducted below Caribbean, FARc and NAZ; subduction of Farallon/Nazca lithosphere below South America following northward movement of Caribbean plate.

4.1.3 This study

In this study, east-dipping subduction beneath the South American margin was interrupted by the opening of the Quebradagrande back-arc at 145 Ma, inducing the detachment of the Farallon (FARa) slab earlier than Boschman et al. (2014). As the back-arc opened, subducting Farallon lithosphere (FARb) initially became smeared along the mantle transition zone as the subduction hinge rolled back (Fig. 8). A polarity reversal associated with the closure of the Quebradagrande back-arc (QB) shows a similar pattern of lateral deflection at the limit between the upper and lower mantle (660 km depth). Subducted oceanic lithosphere associated with the inception of east-dipping subduction at 85 Ma responsible for the isolation of the Caribbean plate sank vertically through the mantle transition zone (FARc; Fig 8). As this material sank it coalesced with the older back-arc sinking slab, continuing to sink as a single thermal anomaly to ~1500-2300 km depth at present between ~85-75°W (Fig. 8).

Because a low convergence rate was assigned between the Proto-Caribbean and the leading edge of the Caribbean plate, based on a kinematic analysis (Fig. 9), there was no significant volume of material prior to ~110 Ma in the model based on our reconstruction. Resumed subduction along the South American margin (FARd and NAZ) that continued to the present day is responsible for mid- to upper-mantle slab material (1500-500 km) predicted at 80-60°W.

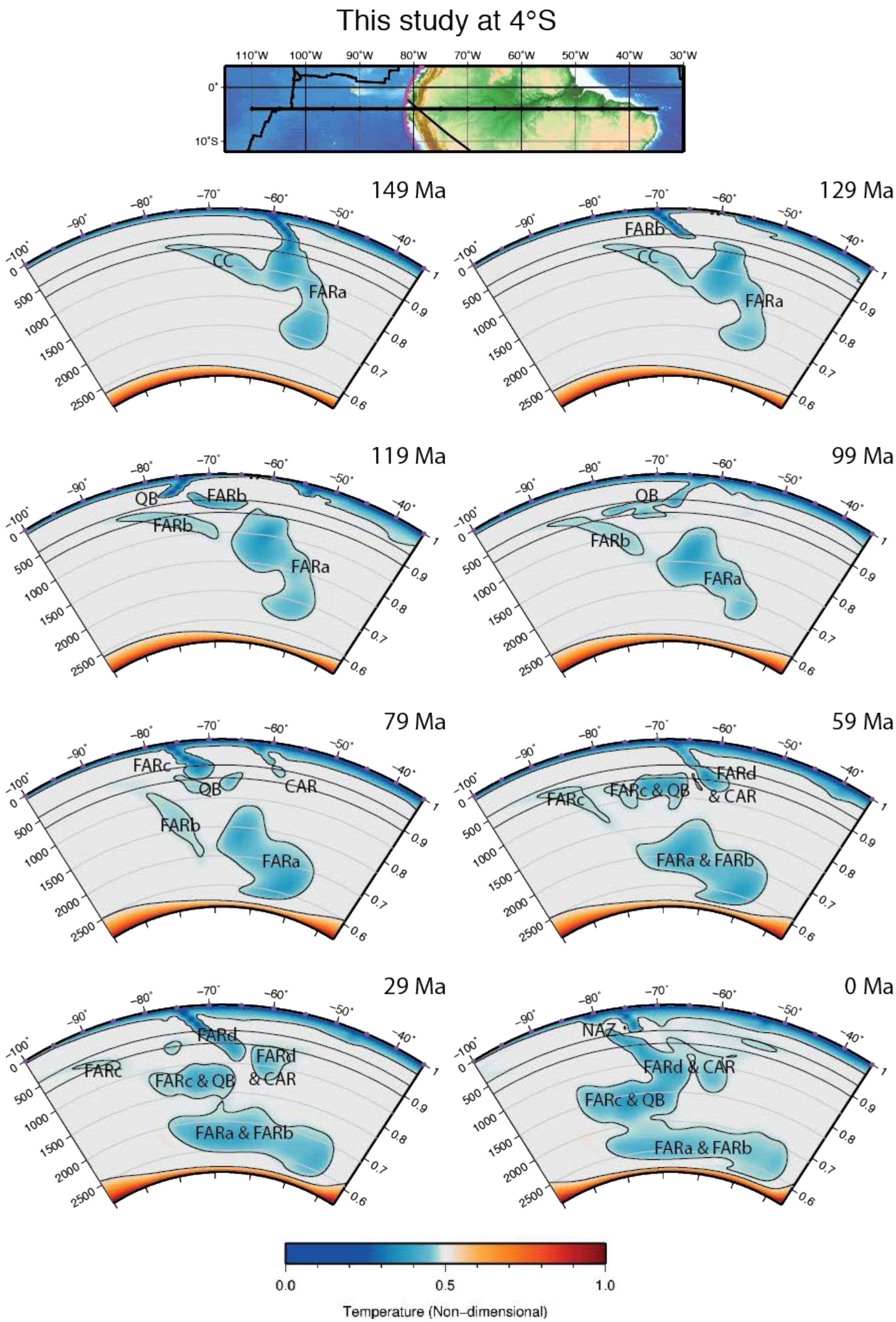

This study at 4°S
149 Ma
129 Ma
119 Ma
99 Ma
79 Ma
59 Ma
29 Ma
0 Ma
CC
FARa
FARb
QB
FARc
CAR
FARc & QB
FARd
& CAR
FARa & FARb
FARd & CAR
NAZ
Temperature (Non–dimensional)
0.0
0.5
1.0

Figure 8. Vertical cross sections at 4°S of time-dependent predicted mantle temperature based on our reconstruction. Black contours correspond to material that is 4% cooler than ambient mantle temperature. CAR = eastward dipping subduction of Caribbean lithosphere below South America; CC = Cache Creek plate; FARa = Jurassic-Cretaceous eastward dipping subduction of Farallon lithosphere below South America; FARb = eastward and southward dipping subduction of Farallon lithosphere below the opening Quebradagrande backarc; FARc = eastward dipping subduction of Farallon lithosphere below Caribbean; FARd and NAZ = eastward dipping subduction of Farallon/Nazca lithosphere below South America following northward movement of Caribbean plate; QB = westward dipping subduction of the Quebradagrande backarc basin beneath the Farallon plate (i.e. back-arc basin closure).

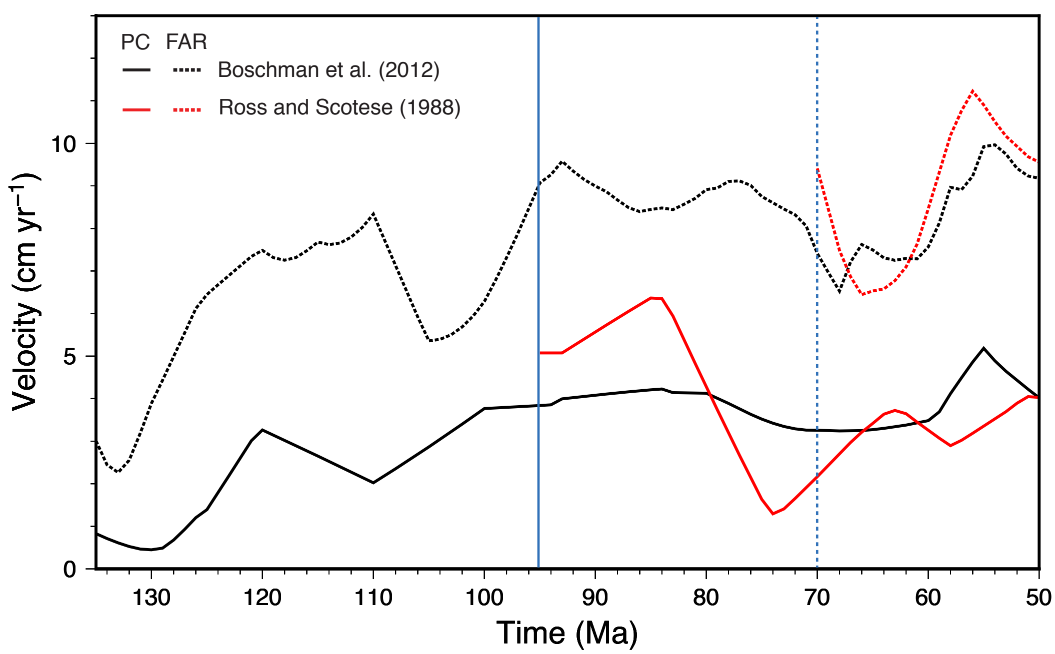

Figure 9. Convergence velocities of the Proto-Caribbean (solid lines) and Farallon plate (dashed lines), relative to the Caribbean plate for Boschman et al. (2014) (assuming that their outboard

plate boundary is a subduction zone) and our model (black) and Ross and Scotese (1988) (red). The onset of westward-dipping subduction of the proto-Caribbean did not occur until 95 Ma (solid blue) in Ross and Scotese (1988), with eastward dipping subduction of Farallon lithosphere below the newly formed Caribbean plate not occurring until 70 Ma (dashed blue).

5. Seismic tomography

Anomalously fast seismic velocities are generally inferred to be representative of cold subducted material based on a first order interpretation of the relationship between seismic wave velocity and temperature. In this section we compare tectonic reconstructions and geodynamic models to horizontal and vertical slices of P- and S-wave tomography models. We selected two P-wave (Li et al., 2008; Montelli et al., 2004) and two S-wave (Grand, 2002; Ritsema et al., 2011) models to visualize the mantle structure in the area. P-wave models allow for high-resolution imaging of subduction zones due to the high concentration of receiver stations in proximity to seismic wave sources, whereas S-wave models provide better coverage of large wavelength features due to the sampling of broadband data (Romanowicz, 2003).

Assuming subducted material sinks largely vertical through the mantle (van der Meer et al., 2010), we can interpret laterally continuous positive seismic anomalies to represent the paleo-location of subduction zones in eastern Panthalassa. We used two alternative sinking rates for the mantle, one with the whole mantle rate of 1.3 cm yr^{-1} (Butterworth et al., 2014) (Fig. 10 and S2-4) (preferred rate) and another that assumes an upper mantle sinking rate of 4.8 cm yr^{-1} derived from Lithgow-Bertelloni and Richards (1998) and a lower-mantle average sinking rate of 1.2 cm yr^{-1} as determined by van der Meer et al. (2010) (Figs. S1). Using these parameters, we converted horizontal depth slices into age to give an approximate age-depth relationship to subducted material. The larger sinking rate adopted for the less viscous upper mantle predicts slabs to be at a greater depth than estimated in van der Meer et al. (2010) and that predicted by our mantle convection models (Fig. 8).

The long-lived continuous subduction zone extending along the western margin of North and South America until 87 Ma proposed by Ross and Scotese (1988) shows a poor correlation with the observed lateral distribution of subducted slab material (Fig. 10). The presence of a subduction zone outboard of the Americas included in Boschman et al. (2014) and our model provide a better fit at depths between 1000-1500 km (Fig. 10). In our reconstructions, we explain the presence of this material as a consequence of the rolling back of the subduction slab associated with both the opening and closing of the Quebradagrande backarc (e.g. at 1,333 km depth; Fig. 10). This is in contrast to the Boschman et al. (2014) reconstruction, which does not propose a subduction zone to explain the presence of the broad region of seismically fast material in the lower mantle.

After 90 Ma, at depths shallower than ~1,100 km, a large volume of subducted slab material close to the equator is present in all the seismic tomography models, marking a northward shift in subduction (Fig. 10). This corresponds well with the location of subduction from 85 Ma in Boschman et al. (2014) and consequently our model, as the Caribbean plate moves into the widening gap between the North and South American continents. The Ross and Scotese (1988) model cannot account for the presence of this material due to a 25 million year delay in the inception of a new western subduction zone isolating the Caribbean plate, relative to the other two models.

In the northern Pacific Ocean basin, which is outside of the scope of this study, seismic anomalies are not well matched by subduction systems. However, the incorporation of intra-oceanic subduction systems outboard of the western North American margin, as in Sigloch and Mihalynuk (2013), may improve correlations in this area as well as the continuity with the subduction systems further south. There may also be scope to improve the shape of the subduction zone at ~80 Ma as it transitioned from an intra-oceanic subduction zone to a subduction zone associated with the Caribbean and the Andean margin (Fig. 10).

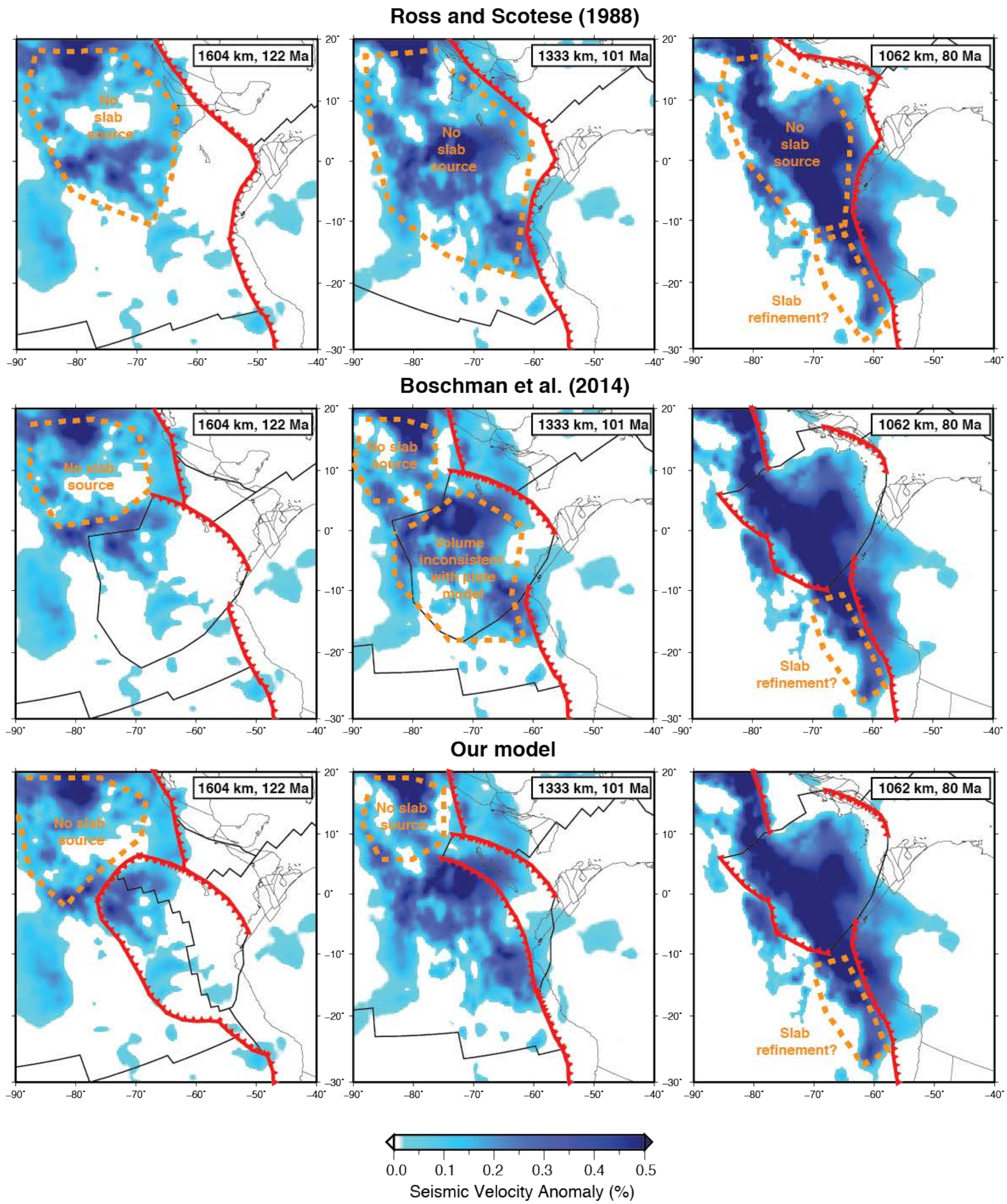

569

570 **Figure 10.** Three alternative plate reconstructions tested in this paper with age-coded seismic

571 tomography depth slices (positive values only) based on MIT-P (Li et al., 2008). Sinking rate used

for the age-coding is a constant rate of 1.3 cm yr^{-1}. Red lines with teeth denote subduction zones, thick black lines denote mid-ocean ridges and transform faults and thin black lines denote coastlines. Dashed orange polygons highlight areas where the plate model and seismic tomography are inconsistent (see text for discussion).

The predicted mantle structure derived from our geodynamic models is also compared to the distribution of seismically fast material in vertical tomography slices.

At mid-mantle depths, the geodynamic models match both P- and S-wave tomography at latitudes between ~5°N and ~10°S (Fig. 11 and Fig. S1-2), in the models where a subduction zone outboard of South America is introduced during the Early Cretaceous. Geodynamic models based on the reconstruction of Boschman et al. (2014) and our new reconstruction account for seismically fast material at depths of ~1,000-2,000 km at ~70-85°W (Fig. 11 and Fig. S1-2). Based on an analysis of the time-dependent mantle temperature, we attribute this material to the subduction of Farallon lithosphere at the western Caribbean margin from 135 Ma in the Boschman et al. (2014) model. Alternatively, in the model based on our new reconstruction, a similar volume of material is sourced from the subduction of Farallon lithosphere at the retreating subduction zone associated with the opening of the Quebradagrande back-arc at 145 Ma, and subsequent subduction of its oceanic crust during basin closure from 120-100 Ma. The model based on the reconstruction by Ross and Scotese (1988) does not replicate this mid-mantle material beneath South America, instead producing a continuous slab extending from ~500 km at ~75°W to the core mantle boundary at ~50°W, that does not correspond to any strong positive anomalies below ~1,500 km depth.

The geodynamic models based on both the reconstruction of Boschman et al. (2014) and our new reconstruction also predict a diagonal slab volume from ~80-60°W at shallower depths of ~500-1,500 km that matches observed positive seismic anomalies imaged in tomography at these latitudes (Fig. 11 and Fig. S1-2). This material was sourced from the Late Cretaceous resumption of subduction of Farallon lithosphere beneath the South American margin. At more southern latitudes (18°S), beneath Peru, all three models predict the near vertical region of high velocity material centred at ~60°W observed in tomography. However, this material is poorly resolved in MIT-P, particularly at depths below ~1,500 km. Faccenna et al. (2017) proposed that a thick slab associated with the subduction of old oceanic lithosphere only penetrated and anchored into the lower mantle ~ 50 ±10 Myr ago at ~20ºS, leading to Andean mountain building. Nevertheless, there is geological evidence from Peru and northern Chile of a continuous record of arc magmatism since the Mesozoic (Scheuber et al., 1994) and geological evidence for orogenesis by the mid-Late Cretaceous (Cobbold et al., 2007; McQuarrie et al., 2005). In addition, the seismic tomography models presented in van der Meer (2017) show a continuous slab from the trench to 2,400-2,800 km depth in southern Peru.

The greatest mismatch between modelled present-day mantle temperature structure and seismic tomography arises in the lower-most mantle > ~2,000 km depth (Fig. 11 and Fig. S1-2). A linear zone of high velocity material in the lower mantle, extending ~30°N and S of the equator (Fig. 10), is present in both P- and S-wave models that is not captured well by the numerical models. This high-velocity volume has previously been identified (Hutko et al., 2006; Kito et al., 2008; Thomas et al., 2004) and interpreted as the result of folding and westward spreading of the Farallon slab at the core mantle boundary (Hutko et al., 2006). van der Meer et al. (2010) identified the same anomaly at depths of 2815-2300 km in the P-wave tomography model of Amaru (2007), instead suggesting that it may be derived from a north-south trending intra-oceanic subduction zone active in eastern Panthalassa during the early Mesozoic (max: 219±11 Ma, min: 178±15 Ma).

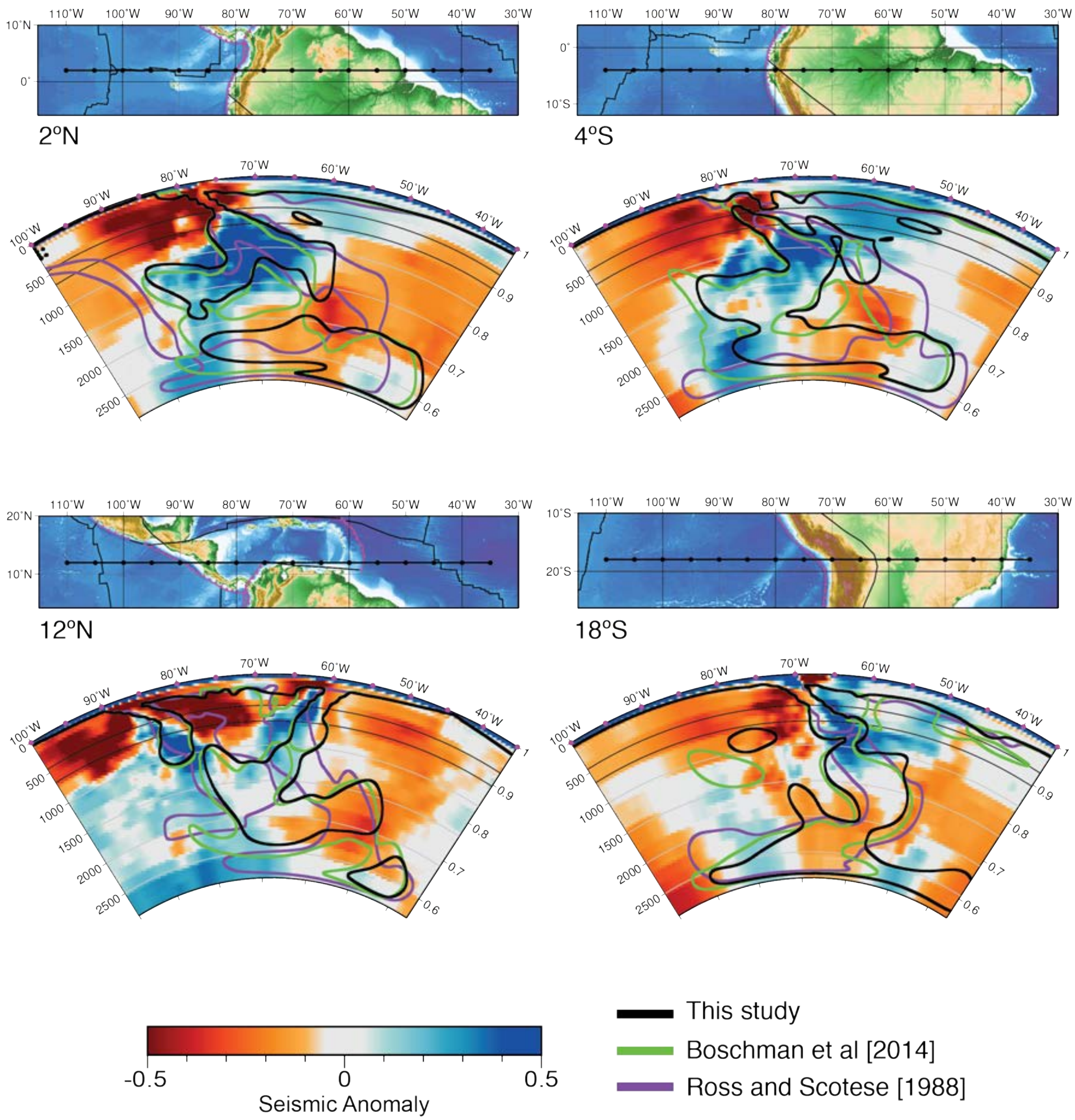

Figure 11. Vertical cross sections of MIT-P seismic tomography model and temperature contours showing mantle 4% cooler than ambient for each model. See Fig. S1-2 for comparison with alternative seismic tomography models.

Folding of the slab, however, is consistent with the behavior observed in the geodynamic models. In the mantle convection models, subduction is modelled for 70 Myr prior to our study period to capture pre-existing mantle heterogeneity. Pre-existing subducted material at ~55°W corresponds to Farallon subduction prior to 150 Ma (slab FARa). In lieu of trench roll-back and slab break-off, continued subduction at ~55°W, albeit with a reversed polarity in the reconstruction of Boschman et al. (2014), supplied additional material to the remnant Farallon slab. The greater volume of subducted material ultimately sank to greater depths, extending laterally along the core-mantle boundary (Fig. 11 and Fig. S1-2). In all model scenarios, this spreading of the Farallon slab in the lower mantle produces a ~500-800 km thick lateral 'blanket' of slab material at the core mantle boundary extending to ~40°W that is largely absent in seismic tomography. This could reflect that too much subducted material is initially present in the convection models, and/or that lower mantle subducted volumes are over-predicted in incompressible flow models. This lower mantle volume is somewhat better resolved in long-wavelength S-wave models. The thermal assimilation over time was proposed by van der Meer et al. (2012) to account for the tomographic indivisibility of slabs in the lower mantle.

6. Discussion

Assuming a first-order relationship between thermal heterogeneities in the mantle and seismic wave velocity, the position of subducted slab material in the mid mantle is replicated by the numerical models when a subduction zone is included outboard of the South American margin during the Early Cretaceous. Additionally, the numerical models show that a long-lived Andean style subduction zone persisting throughout the Mesozoic until ~90 Ma produces the poorest fit to the observed distribution of seismically fast material at the present day beneath western South

America. It therefore seems likely that a subduction zone active during the Early Cretaceous to the west of South America existed and such a subduction zone is necessary to account for the present-day mantle structure. As the model based on the reconstruction of Ross and Scotese (1988) does not reproduce any of the mid-mantle material at ~75-85°W, we consider this model to be the least representative model for this particular aspect of the eastern Panthalassa margin during the early Cretaceous. Focusing on mid-mantle depths, where the geodynamic models best fit seismic tomography, we attempt to distinguish between the possible mechanisms responsible for the types of subduction described by our models and assess their feasibility.

6.1. Subduction initiation in the proto-Pacific

Boschman et al. (2014) constrained the western margin of the Caribbean plate at 135 Ma by the appearance of an unknown plate boundary. A kinematic analysis of convergence rates at this boundary when incorporated into the global model of Müller et al. (2016) (Fig. 9) suggests that this plate boundary was a subduction zone. Models based on our reconstruction produce mid-mantle slab volumes that match seismic tomography. Additionally, for west-dipping subduction of the Proto-Caribbean to have occured from 135 Ma, for which there is evidence (Rojas-Agramonte et al., 2011), the rapid eastward motion of the Farallon plate at this time necessitates the presence of an additional eastward dipping subduction zone consuming Farallon lithosphere. This implies a spontaneous intra-oceanic subduction zone initiation at 135 Ma.

Subduction initiation is a key tectonic process that remains poorly understood (Stern, 2004). Spontaneous subduction initiation is thought to result from gravitational instability of the oceanic lithosphere, whereas for induced subduction initiation, existing plate motions cause compression and lithospheric rupture (Stern, 2004). Transform faults and fracture zones have traditionally been thought to be favorable sites for intra-oceanic subduction initiation (Mueller and Phillips, 1991). Previous numerical models (e.g. Hall et al. (2003)) showed that plate convergence is typically required for inducing subduction initiation at transform faults. Leng and Gurnis (2015), however, showed that spontaneous subduction initiation is possible at transform faults where a greater thermal and compositional density contrast exists, such as where relic arcs are adjacent to old oceanic lithosphere. Thermal rejuvenation of the relic arc causes a reduction in the overriding plate strength leading to the spontaneous initiation of subduction at such sites (Leng and Gurnis, 2015). Recent work has investigated plume-induced subduction in the Caribbean region (Gerya et al., 2015; Whattam and Stern, 2015) whereby subduction is induced along the weak plume head-cold lithosphere interface (Whattam and Stern, 2015).

Despite the theoretical potential of a western Caribbean subduction zone that may have initiated in this spontaneous manner to replicate mid-mantle thermal anomalies, geological evidence for intraoceanic subduction initiation at 135 Ma is lacking. The earliest evidence of arc magmatism preserved in the Panama–Chocó block, located at the inferred subduction boundary, is of Campanian (~83.5-70.6 Ma) age (Denyer et al., 2006; Buchs et al., 2010). Radiolarites intercalated with arc-derived material on the Nicoya peninsula are middle Turonian–Santonian and Coniacian–Santonian in age (Bandini et al., 2008), consistent with Central American subduction initiation at ~85 Ma predicted in both models. However, as previously discussed, there is evidence for the formation of an Early Cretaceous back-arc basin, of unknown extent, along the Northern Andean margin. This scenario involves back-arc basin extension and trench roll back, which is a geodynamically common process, rather than requiring intra-oceanic subduction initiation.

6.2. Cretaceous back-arc basin opening offshore South America and the Caribbean

A key driver in the development of mafic-floored back-arc basins is the rollback of the subduction hinge, expressed through the velocity of trench migration at a subduction zone (Schellart, 2008). A number of studies have also shown that the absolute motion of the overriding plate has an effect on the tectonic regime that arises at the subduction margin (Maloney et al., 2013; Oncken et al., 2006; Ramos, 2010; Sdrolias and Müller, 2006). In these models, seismic decoupling occurs at the trench when the overriding plate is moving away from the subduction hinge inducing an extensional state of stress and leading to the development of back-arc spreading (Sdrolias and Müller, 2006). While some geodynamic modelling studies conclude that the overriding plate motion is a minor contributor to back-arc extension (Chen et al., 2016; Schellart, 2008), others propose that the forces driving the overriding plate away from the trench are necessary to generate back-arc extension, even within the framework of slab rollback (Nakakuki and Mura, 2013). Uyeda and Kanamori (1979) proposed that strong mechanical coupling at subduction zone interfaces is linked to the formation of Cordilleran mountain belts, while weak coupling is associated with back-arc basin formation.

Maloney et al. (2013) calculated negative trench normal convergence rates in the northern Andean region during the Late Jurassic through Early Cretaceous, indicative of motion away from the subduction hinge. This suggests that the conditions necessary for back-arc basin formation existed in this region, and is consistent with evidence of back-arc basin formation preserved in the Colombian and Ecuadorian Andes (Nivia et al., 2006; Villagómez et al., 2011). This provides additional support for the presence of a back-arc basin as implemented in our model. The age of oceanic lithosphere being subducted, and the angle at which it is dipping into the upper mantle, are secondary parameters contributing to trench rollback. It has been shown that back-arc basins may only develop where lithosphere is older than 50-55 Myr, with a minimum slab dip of 30°, (Maloney et al., 2013; Sdrolias and Müller, 2006). Our reconstructed seafloor age-grids show Farallon oceanic lithosphere older than 50 Myr was subducting at the northern Andean margin 145 Myr ago, thus satisfying this condition. Rollback of the subduction hinge dominates the continued creation of accommodation space required for back-arc spreading during the development of the Andean back-arc basins. The closure of these basins in our new reconstruction is associated with increased spreading rates in the South Atlantic Ocean.

Another geodynamic consideration is the along-strike subduction evolution along the Andean margin. Trench rollback resulting in full crustal breakup and subsequent back-arc spreading is restricted to the northernmost part of the proposed Andean back-arc basin in our reconstruction. Crustal extension in the Peruvian and Chilean Andes was insufficient to generate new oceanic crust (Mpodozis and Allmendinger, 1993; Petford and Atherton, 1994; Ramos, 2010). Whilst beyond the geographical scope of this study, the Rocas Verdes back-arc basin of the southernmost Andes is proposed to have been active at approximately the same time as our modelled Northern Andean back-arc. The Rocas Verdes Basin was floored by tholeiitic to transitional type-basalts typical of a back-arc environment (Stern et al., 1976). It opened at 152-142 Ma (Calderón et al., 2007) with rifting propagating northward (Malkowski et al., 2016). The change to a compressional regime and closure of the back arc is similarly attributed to the beginning of westward absolute motion of South America circa 100 Ma (Maloney et al., 2013; Ramos, 2010; Somoza and Zaffarana, 2008).

The development of back-arc basins at only the northern and southernmost regions of the Andean subduction zone, as presented in this study, is consistent with a recent dynamic, buoyancy-driven, whole-mantle subduction model (Schellart, 2017) and the study of Schellart et al. (2007), which explained this phenomenon as a function of lateral slab width. Return flow of mantle material around the edges of retreating subducting slabs facilitates further rapid slab rollback and thus increased lithospheric extension at the edges of long subduction zones > 4,000 km. Away from the edges of such a subduction zone, a central stagnation zone forms where there is a limited opportunity for the upper mantle to flow horizontally around the retreating slab. Ultimately this produces a subduction zone with an overall convex-shaped trench with concave shaped edges, folding around the upper mantle stagnation zone. The shape of our retreating back-arc subduction zone in our model aligns with the inferences made by both Schellart (2017) and (Schellart et al., 2007). Additionally, this effect may explain why extension along the Peruvian and Chilean sections of the Andean margin did not experience full crustal break-up and development of back-arc basins floored by oceanic crust. As well as explaining the opening of the Rocas Verdes and Quebradagrande back-arc basins over several million years, the model of Schellart (2017) also explains our modelled progressive closure of the Andean back-arc basins, which would have led to subsequent shortening and orogenesis along the South American active margin. We therefore consider subduction outboard of South America as the retreating subduction margin of a back-arc basin to provide a better fit for observed mid-mantle high velocity material, better reflect the observed geology and can be explained by previously published models on subduction and back-arc basin behavior.

7. Conclusion

We used geodynamic models driven by surface plate reconstructions to compare alternative subduction histories to present-day tomographic images of the mantle structure. We constrained the location and evolution of subduction in eastern Panthalassa adjacent to South America during the Cretaceous. Our kinematic and numerical modelling results show that subduction located outboard of the South American margin during the Early Cretaceous matches the observed lateral and vertical distribution of slab material in seismic tomography at mid-mantle depths (500-2,000 km). When no such subduction zone is included, geodynamic models cannot account for the westernmost seismic anomalies beneath South America. We therefore constrain the location of Early Cretaceous subduction to be 15-20° west of the South American continental margin.

We show that this subduction zone was likely associated with the formation of a back-arc basin in response to trench roll back at 145 Ma rather than spontaneous intra-oceanic subduction formation. This interpretation is consistent with geological evidence of Cretaceous back-arc basin formation and terrane accretion preserved on the present-day Northern Andean margin. We consider the opening of this basin to be the northern expression of a major phase of extension along the Andean margin, coeval with extensive crustal thinning in the Peruvian Andes. Our model of two Jurassic-Cretaceous wedge-shaped back-arc basins forming along the Andes and their subsequent closure is consistent with the subduction dynamics of the Andean margin based on an independently-derived geodynamic model (Schellart, 2017). Further work on extending the continuity of this subduction zone to the north (adjacent to the western margin of North America) and to the south (along the entire South American margin) will help resolve the subduction history of eastern Panthalassa, with implications for mantle dynamics and the location of LLSVPs, geochemical cycles that are influenced by the amount of material subducted into the mantle and long-term sea-level change related to the volume of the ocean basins.

Acknowledgments

This research was undertaken with the assistance of the Sydney Informatics Hub in accessing resources from the National Computational Infrastructure (NCI), which is supported by the Australian Government. The authors were supported by Australian Research Council grants IH130200012 (RDM, NF), FT130101564 (MS) and DE160101020 (NF). We would like to thank Wouter Schellart and an anonymous reviewer for their helpful comments, which improved the manuscript.

References

Alpert, L.A., Becker, T.W., Bailey, I.W., 2010. Global slab deformation and centroid moment tensor constraints on viscosity. Geochemistry, Geophysics, Geosystems 11.

Amante, C., Eakins, B., Boulder, C., 2009. ETOPO1 1 arc-minute global relief model: Procedures, data sources and analysis. NOAA Technical Memorandum.

Amaru, M., 2007. Global travel time tomography with 3-D reference models. Geologica Ultraiectina 274.

Atherton, M.P., 1990. The Coastal Batholith of Peru: The product of rapid recycling of 'new' crust formed within rifted continental margin. Geological Journal 25, 337-349.

Atherton, M.P., Aguirre, L., 1992. Thermal and geotectonic setting of Cretaceous volcanic rocks near Ica, Peru, in relation to Andean crustal thinning. Journal of South American Earth Sciences 5, 47-69.

Atherton, M.P., Webb, S., 1989. Volcanic facies, structure, and geochemistry of the marginal basin rocks of central Peru. Journal of South American Earth Sciences 2, 241-261.

Bird, P., 2003. An updated digital model of plate boundaries. Geochemistry, Geophysics, Geosystems 4.

Boschman, L.M., van Hinsbergen, D.J.J., Torsvik, T.H., Spakman, W., Pindell, J.L., 2014. Kinematic reconstruction of the Caribbean region since the Early Jurassic. Earth-Science Reviews 138, 102-136.

Bouysse, P., 1988. Opening of the Grenada back-arc Basin and evolution of the Caribbean plate during the Mesozoic and early Paleogene. Tectonophysics 149, 121-143.

Bower, D.J., Gurnis, M., Flament, N., 2015. Assimilating lithosphere and slab history in 4-D Earth models. Physics of the Earth and Planetary Interiors 238, 8-22.

Burke, K., 1988. Tectonic Evolution of the Caribbean. Annual Review of Earth and Planetary Sciences 16, 201-230.

Butterworth, N., Talsma, A., Müller, R., Seton, M., Bunge, H.-P., Schuberth, B., Shephard, G., Heine, C., 2014. Geological, tomographic, kinematic and geodynamic constraints on the dynamics of sinking slabs. Journal of Geodynamics 73, 1-13.

Calderón, M., Fildani, A., Hervé, F., Fanning, C.M., Weislogel, A., Cordani, U., 2007. Late Jurassic bimodal magmatism in the northern sea-floor remnant of the Rocas Verdes basin, southern Patagonian Andes. Journal of the Geological Society 164, 1011-1022.

Chase, C.G., 1978. Extension behind island arcs and motions relative to hot spots. Journal of Geophysical Research: Solid Earth 83, 5385-5387.

Chen, Z., Schellart, W.P., Strak, V., Duarte, J.C., 2016. Does subduction-induced mantle flow drive backarc extension? Earth and Planetary Science Letters 441, 200-210.

Cobbing, E., 1978. The Andean geosyncline in Peru, and its distinction from Alpine geosynclines. Journal of the Geological Society 135, 207-218.

Cobbold, P.R., Rossello, E.A., Roperch, P., Arriagada, C., Gómez, L.A., Lima, C., 2007. Distribution, timing, and causes of Andean deformation across South America. Geological Society, London, Special Publications 272, 321-343.

Cochrane, R., 2013. U-Pb thermochronology, geochronology and geochemistry of NW South America: rift to drift transition, active margin dynamics and implications for the volume balance of continents. University of Geneva.

Cochrane, R., Spikings, R., Gerdes, A., Winkler, W., Ulianov, A., Mora, A., Chiaradia, M., 2014. Distinguishing between in-situ and accretionary growth of continents along active margins. Lithos 202–203, 382-394.

Dalziel, I.W.D., de Wit, M.J., Palmer, K.F., 1974. Fossil marginal basin in the southern Andes. Nature 250, 291-294.

Domeier, M., Doubrovine, P.V., Torsvik, T.H., Spakman, W., Bull, A.L., 2016. Global correlation of lower mantle structure and past subduction. Geophysical Research Letters 43, 4945-4953.

Duncan, R.A., Hargraves, R.B., 1984. Plate tectonic evolution of the Caribbean region in the mantle reference frame. Geological Society of America Memoirs 162, 81-94.

Eagles, G., 2007. New angles on South Atlantic opening. Geophysical Journal International 168, 353-361.

Faccenna, C., Funiciello, F., Giardini, D., Lucente, P., 2001. Episodic back-arc extension during restricted mantle convection in the Central Mediterranean. Earth and Planetary Science Letters 187, 105-116.

Faccenna, C., Oncken, O., Holt, A.F., Becker, T.W., 2017. Initiation of the Andean orogeny by lower mantle subduction. Earth and Planetary Science Letters 463, 189-201.

Flament, N., Gurnis, M., Müller, R.D., Bower, D.J., Husson, L., 2015. Influence of subduction history on South American topography. Earth and Planetary Science Letters 430, 9-18.

Flament, N., Gurnis, M., Williams, S., Seton, M., Skogseid, J., Heine, C., Dietmar Müller, R., 2014. Topographic asymmetry of the South Atlantic from global models of mantle flow and lithospheric stretching. Earth and Planetary Science Letters 387, 107-119.

Flament, N., Williams, S., Müller, R., Gurnis, M., Bower, D.J., 2017. Origin and evolution of the deep thermochemical structure beneath Eurasia. Nature communications 8, 14164.

García-Casco, A., Torres-Roldán, R., Iturralde-Vinent, M.A., Millán, G., Cambra, K.N., Lázaro, C., Vega, A.R., 2006. High pressure metamorphism of ophiolites in Cuba. Geologica Acta: an international earth science journal 4, 63-88.

Gerya, T.V., Stern, R.J., Baes, M., Sobolev, S.V., Whattam, S.A., 2015. Plate tectonics on the Earth triggered by plume-induced subduction initiation. Nature 527, 221-225.

Gerya, T.V., Stöckhert, B., Perchuk, A.L., 2002. Exhumation of high-pressure metamorphic rocks in a subduction channel: A numerical simulation. Tectonics 21.

González, H., 1980. Geologia de la planchas 167 (Sonson) y 187 (Salamina)(escala 1: 100,000). Instituto Nacional de Investigaciones Geológico-Mineras.

Grand, S.P., 2002. Mantle shear–wave tomography and the fate of subducted slabs. Philosophical Transactions of the Royal Society of London A: Mathematical, Physical and Engineering Sciences 360, 2475-2491.

Gurnis, M., Turner, M., Zahirovic, S., DiCaprio, L., Spasojevic, S., Müller, R.D., Boyden, J., Seton, M., Manea, V.C., Bower, D.J., 2012. Plate tectonic reconstructions with continuously closing plates. Computers & Geosciences 38, 35-42.

Hall, C.E., Gurnis, M., Sdrolias, M., Lavier, L.L., Müller, R.D., 2003. Catastrophic initiation of subduction following forced convergence across fracture zones. Earth and Planetary Science Letters 212, 15-30.

Hastie, A.R., Kerr, A.C., Mitchell, S.F., Millar, I.L., 2009. Geochemistry and tectonomagmatic significance of Lower Cretaceous island arc lavas from the Devils Racecourse Formation, eastern Jamaica. Geological Society, London, Special Publications 328, 339-360.

Hawkins, J.W., 1995. The Geology of the Lau Basin, in: Taylor, B. (Ed.), Backarc Basins: Tectonics and Magmatism. Springer US, Boston, MA, pp. 63-138.

Hernlund, J.W., Houser, C., 2008. On the statistical distribution of seismic velocities in Earth's deep mantle. Earth and Planetary Science Letters 265, 423-437.

Heuret, A., Lallemand, S., 2005. Plate motions, slab dynamics and back-arc deformation. Physics of the Earth and Planetary Interiors 149, 31-51.

Hutko, A.R., Lay, T., Garnero, E.J., 2006. Seismic detection of folded, subducted lithosphere at the core-mantle boundary. Nature [H.W. Wilson - GS] 441, 333.

James, K.H., 2005. Arguments for and against the Pacific origin of the Caribbean Plate and arguments for an in situ origin. Caribbean Journal of Earth Science 39, 47-67.

James, K.H., 2009. In situ origin of the Caribbean: discussion of data. Geological Society, London, Special Publications 328, 77-125.

Jaramillo, J., Cardona, A., León, S., Valencia, V., Vinasco, C., 2017. Geochemistry and geochronology from Cretaceous magmatic and sedimentary rocks at 6° 35′ N, western flank of the Central cordillera (Colombian Andes): Magmatic record of arc growth and collision. Journal of South American Earth Sciences 76, 460-481.

Johnston, S.T., Borel, G.D., 2007. The odyssey of the Cache Creek terrane, Canadian Cordillera: Implications for accretionary orogens, tectonic setting of Panthalassa, the Pacific superwell, and break-up of Pangea. Earth and Planetary Science Letters 253, 415-428.

Karig, D.E., 1971. Origin and development of marginal basins in the western Pacific. Journal of Geophysical Research 76, 2542-2561.

Kennan, L., Pindell, J.L., 2009. Dextral shear, terrane accretion and basin formation in the Northern Andes: best explained by interaction with a Pacific-derived Caribbean Plate? Geological Society, London, Special Publications 328, 487-531.

Kerr, A.C., Marriner, G.F., Tarney, J., Nivia, A., Saunders, A.D., Thirlwall, M.F., Sinton, C.W., 1997. Cretaceous Basaltic Terranes in Western Columbia: Elemental, Chronological and Sr–Nd Isotopic Constraints on Petrogenesis. Journal of Petrology 38, 677-702.

Kerr, A.C., White, R.V., Thompson, P.M., Tarney, J., Saunders, A.D., 2003. No oceanic plateau—no Caribbean plate? The seminal role of an oceanic plateau in Caribbean plate evolution.

Kito, T., Thomas, C., Rietbrock, A., Garnero, E.J., Nippress, S.E., Heath, A.E., 2008. Seismic evidence for a sharp lithospheric base persisting to the lowermost mantle beneath the Caribbean. Geophysical Journal International 174, 1019-1028.

Leng, W., Gurnis, M., 2015. Subduction initiation at relic arcs. Geophysical Research Letters 42, 7014-7021.

Li, C., van der Hilst, R.D., Engdahl, E.R., Burdick, S., 2008. A new global model for P wave speed variations in Earth's mantle. Geochemistry, Geophysics, Geosystems 9, n/a-n/a.

Lithgow-Bertelloni, C., Richards, M.A., 1998. The dynamics of Cenozoic and Mesozoic plate motions. Reviews of Geophysics 36, 27-78.

Malkowski, M.A., Grove, M., Graham, S.A., 2016. Unzipping the Patagonian Andes—Long-lived influence of rifting history on foreland basin evolution. Lithosphere 8, 23-28.

Maloney, K.T., Clarke, G.L., Klepeis, K.A., Quevedo, L., 2013. The Late Jurassic to present evolution of the Andean margin: Drivers and the geological record. Tectonics 32, 1049-1065.

Matthews, K.J., Williams, S.E., Whittaker, J.M., Müller, R.D., Seton, M., Clarke, G.L., 2015. Geologic and kinematic constraints on Late Cretaceous to mid Eocene plate boundaries in the southwest Pacific. Earth-Science Reviews 140, 72-107.

McQuarrie, N., Horton, B.K., Zandt, G., Beck, S., DeCelles, P.G., 2005. Lithospheric evolution of the Andean fold–thrust belt, Bolivia, and the origin of the central Andean plateau. Tectonophysics 399, 15-37.

Meschede, M., Frisch, W., 1998. A plate-tectonic model for the Mesozoic and Early Cenozoic history of the Caribbean plate. Tectonophysics 296, 269-291.

Montelli, R., Nolet, G., Dahlen, F., Masters, G., Engdahl, E.R., Hung, S.-H., 2004. Finite-frequency tomography reveals a variety of plumes in the mantle. Science 303, 338-343.

Mora-Bohórquez, J.A., Ibánez-Mejia, M., Oncken, O., de Freitas, M., Vélez, V., Mesa, A., Serna, L., 2017. Structure and age of the Lower Magdalena Valley basin basement, northern Colombia: New reflection-seismic and U-Pb-Hf insights into the termination of the central andes against the Caribbean basin. Journal of South American Earth Sciences 74, 1-26.

Moreno-Sanchez, M., Pardo-Trujillo, A., 2003. Stratigraphical and sedimentological constraints on western Colombia: Implications on the evolution of the Caribbean plate, in: Bartolini, C., Buffler, R.T., Blickwede, J.F. (Eds.), The Circum-Gulf of Mexico and the Caribbean: Hydrocarbon habitats, basin formation, and plate tectonics: AAPG Memoir 79, pp. 891-924.

Mpodozis, C., Allmendinger, R.W., 1993. Extensional tectonics, Cretaceous Andes, northern Chile (27°S). Geological Society of America Bulletin 105, 1462-1477.

Mpodozis, C., Ramos, V.A., 1990. The Andes of Chile and Argentina, in: Ericksen, G.E., Pinochet, T.C., Reinemund, J.A. (Eds.). Tulsa, OK (USA); Circum-Pacific Council, pp. 59-90.

Mueller, S., Phillips, R.J., 1991. On the initiation of subduction. Journal of Geophysical Research 96, 651-665.

Müller, R.D., Royer, J.-Y., Cande, S.C., Roest, W.R., Maschenkov, S., 1999. Chapter 2 New constraints on the late cretaceous/tertiary plate tectonic evolution of the caribbean, in: Mann, P. (Ed.), Sedimentary Basins of the World. Elsevier, pp. 33-59.

Müller, R.D., Sdrolias, M., Gaina, C., Roest, W.R., 2008. Age, spreading rates, and spreading asymmetry of the world's ocean crust. Geochemistry, Geophysics, Geosystems 9.

Müller, R.D., Seton, M., Zahirovic, S., Williams, S.E., Matthews, K.J., Wright, N.M., Shephard, G.E., Maloney, K., Barnett-Moore, N., Hosseinpour, M., Bower, D.J., Cannon, J., 2016. Ocean Basin Evolution and Global-Scale Plate Reorganization Events Since Pangea Breakup. Annual Review of Earth and Planetary Sciences 44, null.

Nakakuki, T., Mura, E., 2013. Dynamics of slab rollback and induced back-arc basin formation. Earth and Planetary Science Letters 361, 287-297.

Nerlich, R., Clark, S.R., Bunge, H.-P., 2015. An outlet for Pacific mantle: The Caribbean Sea? GeoResJ 7, 59-65.

Nivia, A., Marriner, G.F., Kerr, A.C., Tarney, J., 2006. The Quebradagrande Complex: A Lower Cretaceous ensialic marginal basin in the Central Cordillera of the Colombian Andes. Journal of South American Earth Sciences 21, 423-436.

Oncken, O., Hindle, D., Kley, J., Elger, K., Victor, P., Schemmann, K., 2006. Deformation of the Central Andean Upper Plate System — Facts, Fiction, and Constraints for Plateau Models, in: Oncken, O., Chong, G., Franz, G., Giese, P., Götze, H.-J., Ramos, V., Strecker, M., Wigger, P. (Eds.), The Andes. Springer Berlin Heidelberg, pp. 3-27.

Petford, N., Atherton, M.P., 1994. Cretaceous-Tertiary volcanism and syn-subduction crustal extension in northern central Peru. Geological Society, London, Special Publications 81, 233-248.

Pindell, J., Dewey, J.F., 1982. Permo-Triassic reconstruction of western Pangea and the evolution of the Gulf of Mexico/ Caribbean region. Tectonics 1, 179-211.

Pindell, J., Maresch, W.V., Martens, U., Stanek, K., 2012. The Greater Antillean Arc: Early Cretaceous origin and proposed relationship to Central American subduction mélanges: implications for models of Caribbean evolution. International Geology Review 54, 131-143.

Pindell, J.L., Barrett, S.F., 1990. Geological evolution of the Caribbean region: a plate tectonic perspective. The Caribbean Region, 405-432.

Pindell, J.L., Kennan, L., 2009. Tectonic evolution of the Gulf of Mexico, Caribbean and northern South America in the mantle reference frame: an update. Geological Society, London, Special Publications 328, 1-55.

Ramos, V.A., 2010. The tectonic regime along the Andes: Present-day and Mesozoic regimes. Geological Journal 45, 2.

Restrepo-Pace, P.A., 1992. Petrotectonic characterization of the Central Andean Terrane, Colombia. Journal of South American Earth Sciences 5, 97-116.

Restrepo-Pace, P.A., Ruiz, J., Gehrels, G., Cosca, M., 1997. Geochronology and Nd isotopic data of Grenville-age rocks in the Colombian Andes: new constraints for Late Proterozoic-Early Paleozoic paleocontinental reconstructions of the Americas. Earth and Planetary Science Letters 150, 427-441.

Ritsema, J., Deuss, a.A., Van Heijst, H., Woodhouse, J., 2011. S40RTS: a degree-40 shear-velocity model for the mantle from new Rayleigh wave dispersion, teleseismic traveltime and normal-mode splitting function measurements. Geophysical Journal International 184, 1223-1236.

Rojas-Agramonte, Y., Kröner, A., García-Casco, A., Somin, M., Iturralde-Vinent, M., Mattinson, J., Trujillo, G.M., Sukar, K., Rodríguez, M.P., Carrasquilla, S., 2011. Timing and evolution of Cretaceous island arc magmatism in central Cuba: implications for the history of arc systems in the northwestern Caribbean. The Journal of Geology 119, 619-640.

Romanowicz, B., 2003. Global mantle tomography: progress status in the past 10 years. Annual Review of Earth and Planetary Sciences 31, 303-328.

Rosencrantz, E., Ross, M.I., Sclater, J.G., 1988. Age and spreading history of the Cayman Trough as determined from depth, heat flow, and magnetic anomalies. Journal of Geophysical Research: Solid Earth (1978–2012) 93, 2141-2157.

Ross, M., Rosencrantz, E., Scotese, C., Barrett, S., 1986. Caribbean plate reconstructions: New interpretation of data in the Cayman Trough, Mesozoic and Cenozoic Plate Reconstructions, Geodyn Symp (abstr) Ross M, Scotese C (1988) A hierarchical tectonic model of the Gulf of Mexico and Caribbean region. Tectonophysics, pp. 139-168.

Ross, M.I., Scotese, C.R., 1988. A hierarchical tectonic model of the Gulf of Mexico and Caribbean region. Tectonophysics 155, 139-168.

Sarmiento-Rojas, L.F., Van Wess, J.D., Cloetingh, S., 2006. Mesozoic transtensional basin history of the Eastern Cordillera, Colombian Andes: Inferences from tectonic models. Journal of South American Earth Sciences 21, 383-411.

Schellart, W., 2008. Subduction zone trench migration: Slab driven or overriding-plate-driven? Physics of the Earth and Planetary Interiors 170, 73-88.

Schellart, W., 2017. Andean mountain building and magmatic arc migration driven by subduction-induced whole mantle flow. Nature communications 8, 2010.

Schellart, W.P., Freeman, J., Stegman, D.R., Moresi, L., May, D., 2007. Evolution and diversity of subduction zones controlled by slab width. Nature 446, 308-311.

Schellart, W.P., Lister, G.S., Toy, V.G., 2006. A Late Cretaceous and Cenozoic reconstruction of the Southwest Pacific region: Tectonics controlled by subduction and slab rollback processes. Earth-Science Reviews 76, 191-233.

Schellart, W.P., Moresi, L., 2013. A new driving mechanism for backarc extension and backarc shortening through slab sinking induced toroidal and poloidal mantle flow: Results from dynamic subduction models with an overriding plate. Journal of Geophysical Research: Solid Earth 118, 3221-3248.

Scheuber, E., Bogdanic, T., Jensen, A., Reutter, K.-J., 1994. Tectonic development of the north Chilean Andes in relation to plate convergence and magmatism since the Jurassic, Tectonics of the southern central Andes. Springer, pp. 121-139.

Sdrolias, M., Müller, R.D., 2006. Controls on back-arc basin formation. Geochemistry, Geophysics, Geosystems 7.

Sdrolias, M., Müller, R.D., Gaina, C., 2003. Tectonic evolution of the southwest Pacific using constraints from backarc basins. Geological Society of America Special Papers 372, 343-359.

Serrano, L., Ferrari, L., Martínez, M.L., Petrone, C.M., Jaramillo, C., 2011. An integrative geologic, geochronologic and geochemical study of Gorgona Island, Colombia: Implications for the formation of the Caribbean Large Igneous Province. Earth and Planetary Science Letters 309, 324-336.

Seton, M., Müller, R.D., Zahirovic, S., Gaina, C., Torsvik, T., Shephard, G., Talsma, A., Gurnis, M., Turner, M., Maus, S., Chandler, M., 2012. Global continental and ocean basin reconstructions since 200 Ma. Earth-Science Reviews 113, 212-270.

Shephard, G.E., Matthews, K.J., Hosseini, K., Domeier, M., 2017. On the consistency of seismically imaged lower mantle slabs. Scientific Reports 7, 10976.

Shephard, G.E., Müller, R.D., Seton, M., 2013. The tectonic evolution of the Arctic since Pangea breakup: Integrating constraints from surface geology and geophysics with mantle structure. Earth-Science Reviews 124, 148-183.

Sigloch, K., Mihalynuk, M.G., 2013. Intra-oceanic subduction shaped the assembly of Cordilleran North America. Nature 496, 50-56.

Sinton, C.W., Duncan, R., Storey, M., Lewis, J., Estrada, J., 1998. An oceanic flood basalt province within the Caribbean plate. Earth and Planetary Science Letters 155, 221-235.

Soler, P., Bonhomme, M.G., 1990. Relation of magmatic activity to plate dynamics in central Peru from Late Cretaceous to present. Geological Society of America Special Papers 241, 173-192.

Somin, M.L., Arakelyants, M.M., Kolesnikov, E.M., 1992. AGE AND TECTONIC SIGNIFICANCE OF HIGH-PRESSURE METAMORPHIC ROCKS OF CUBA. International Geology Review 34, 105-118.

Somoza, R., Zaffarana, C.B., 2008. Mid-Cretaceous polar standstill of South America, motion of the Atlantic hotspots and the birth of the Andean cordillera. Earth and Planetary Science Letters 271, 267-277.

Spikings, R., Cochrane, R., Villagomez, D., Van der Lelij, R., Vallejo, C., Winkler, W., Beate, B., 2015. The geological history of northwestern South America: from Pangaea to the early collision of the Caribbean Large Igneous Province (290–75 Ma). Gondwana Research 27, 95-139.

Stegman, D.R., Freeman, J., Schellart, W.P., Moresi, L., May, D., 2006. Influence of trench width on subduction hinge retreat rates in 3-D models of slab rollback. Geochemistry, Geophysics, Geosystems 7.

Steinberger, B., Sutherland, R., O'connell, R.J., 2004. Prediction of Emperor-Hawaii seamount locations from a revised model of global plate motion and mantle flow. Nature 430, 167.

Stern, C., de Wit, M.J., Lawrence, J.R., 1976. Igneous and metamorphic processes associated with the formation of Chilean Ophiolites and their implication for ocean floor metamorphism, seismic layering, and magnetism. Journal of Geophysical Research 81, 4370-4380.

Stern, C.R., De Wit, M.J., 2003. Rocas Verdes ophiolites, southernmost South America: remnants of progressive stages of development of oceanic-type crust in a continental margin back-arc basin. Geological Society, London, Special Publications 218, 665-683.

Stern, R.J., 2004. Subduction initiation: spontaneous and induced. Earth and Planetary Science Letters 226, 275-292.

Thomas, C., Garnero, E.J., Lay, T., 2004. High-resolution imaging of lowermost mantle structure under the Cocos plate. Journal of Geophysical Research: Solid Earth 109.

Toussaint, J., Restrepo, J., 1994. The Colombian Andes during Cretaceous times, Cretaceous tectonics of the Andes. Springer, pp. 61-100.

Uyeda, S., Kanamori, H., 1979. Back-arc opening and the mode of subduction. Journal of Geophysical Research: Solid Earth 84, 1049-1061.

Vallejo, C., Spikings, R.A., Luzieux, L., Winkler, W., Chew, D., Page, L., 2006. The early interaction between the Caribbean Plateau and the NW South American Plate. Terra Nova 18, 264-269.

Vallejo, C., Winkler, W., Spikings, R.A., Luzieux, L., Heller, F., Bussy, F., 2009. Mode and timing of terrane accretion in the forearc of the Andes in Ecuador. Geological Society of America Memoirs 204, 197-216.

van Benthem, S., Govers, R., Spakman, W., Wortel, R., 2013. Tectonic evolution and mantle structure of the Caribbean. Journal of Geophysical Research: Solid Earth 118, 3019-3036.

van der Meer, D.G., Spakman, W., van Hinsbergen, D.J.J., Amaru, M.L., Torsvik, T.H., 2010. Towards absolute plate motions constrained by lower-mantle slab remnants. Nature Geosci 3, 36-40.

van der Meer, D.G., Torsvik, T.H., Spakman, W., van Hinsbergen, D.J.J., Amaru, M.L., 2012. Intra-Panthalassa Ocean subduction zones revealed by fossil arcs and mantle structure. Nature Geosci 5, 215-219.

van der Meer, D.G., van Hinsbergen, D.J., Spakman, W., 2017. Atlas of the Underworld: slab remnants in the mantle, their sinking history, and a new outlook on lower mantle viscosity. Tectonophysics.

Vásquez, M., Altenberger, U., 2005. Mid-Cretaceous extension-related magmatism in the eastern Colombian Andes. Journal of South American Earth Sciences 20, 193-210.

Villagómez, D., Spikings, R., Magna, T., Kammer, A., Winkler, W., Beltrán, A., 2011. Geochronology, geochemistry and tectonic evolution of the Western and Central cordilleras of Colombia. Lithos 125, 875-896.

Villagómez Diaz, D., 2010. Thermochronology, geochronology and geochemistry of the Western and Central cordilleras and Sierra Nevada de Santa Marta, Colombia: The tectonic evolution of NW South America. University of Geneva.

Whattam, S.A., Stern, R.J., 2015. Late Cretaceous plume-induced subduction initiation along the southern margin of the Caribbean and NW South America: The first documented example with implications for the onset of plate tectonics. Gondwana Research 27, 38-63.

Williams, S., Flament, N., Müller, R.D., Butterworth, N., 2015. Absolute plate motions since 130 Ma constrained by subduction zone kinematics. Earth and Planetary Science Letters 418, 66-77.

Zhong, S., McNamara, A., Tan, E., Moresi, L., Gurnis, M., 2008. A benchmark study on mantle convection in a 3-D spherical shell using CitcomS. Geochemistry, Geophysics, Geosystems 9.